NASA
Technical
Paper
2376

December 1984

Translational Control of a Graphically Simulated Robot Arm by Kinematic Rate Equations That Overcome Elbow Joint Singularity

L. Keith Barker,
Jacob A. Houck,
and Susan W. Carzoo

NASA

NASA Technical Paper 2376

1984

Translational Control of a Graphically Simulated Robot Arm by Kinematic Rate Equations That Overcome Elbow Joint Singularity

L. Keith Barker
and Jacob A. Houck
Langley Research Center
Hampton, Virginia

Susan W. Carzoo
Sperry Corporation
Hampton, Virginia

National Aeronautics
and Space Administration

Scientific and Technical Information Branch

SYMBOLS

a_i	perpendicular distance between Z_{i-1} and Z_i
E	elbow of robot arm
H	hand of robot arm
H_3	integer used in figure 5 to cause $\theta_3 = \theta_{3,p}$
h	integration step size
i	integer to indicate different axis systems and associated parameters, i = 1,2, ..., 6
$\mathbf{J}_1$	Jacobian matrix relating waist, shoulder, and elbow joint rates to translational velocity commands (in base coordinates) to robot hand
K_3	proportionality constant in equation (7)
k	integer
L	transformation matrix from hand axis system to base axis system
$\mathbf{L}_{ij}$	row and column of **L**
ℓ	perpendicular distance of wrist from line of rotation of waist joint
ℓ_{ES}	length from elbow to shoulder
ℓ_{HW}	length from hand to wrist
ℓ_{NO}	length from neck to base
ℓ_{SN}	length from shoulder to neck
ℓ_{WE}	length from wrist to elbow
ℓ_{WS}	length from wrist to shoulder; changes as elbow bends
M	maximum absolute value of $\dot{\theta}_3$
N	neck of robot arm
O	base of robot arm
P	projection of wrist position onto X_1
$\mathbf{R}_{i-1}^{i}$	rotational transformation matrix from coordinate system i to i - 1
r_i	distance between coordinate systems i - 1 and i along Z_{i-1}
S	shoulder of robot arm
t	time

$\vec{v}$ translational velocity vector

V_T, V_p, V_R linear velocity component in direction of thrust, pitch, or rotation, respectively

V_{X0}, V_{Y0}, V_{Z0} components of translational velocity vector in base axis system

V_{X2}, V_{Y2}, V_{Z2} components of translational velocity vector in axis system X_2, Y_2, Z_2

V_{X6}, V_{Y6}, V_{Z6} components of translational velocity vector of robot hand in hand axis system

W wrist of robot arm

X_0, Y_0, Z_0 base axis system

X_6, Y_6, Z_6 robot hand axis system

α_i angle between Z_{i-1} and Z_i, measured positively about positive X_i

δ_{min} minimum value for δ_3

δ_3, δ_{23} specified positive constant in equations (8) and (28), respectively

θ_i joint angle with initial value corresponding to initial position of robot arm in figure 1

θ_i' joint angle between X_{i-1} and X_i, measured positively counterclockwise about Z_{i-1}

$\theta_i(k)$ value of θ_i at time kh

$\theta_{3,p}$ particular value of θ_3

θ_3^* last θ_3 in resolved-rate branch of computer program prior to entering singular elbow region of robot arm (fig. 5)

ρ angle to indicate pitching motion (fig. 4)

σ angle which is coordinated with θ_3 to extend and retract robot arm along a straight line (fig. 4)

$\omega_{X6}, \omega_{Y6}, \omega_{Z6}$ rotational velocity components of robot hand, expressed in hand axis system (X_6, Y_6, Z_6)

Subscripts:

0 base axis system

6 hand axis system

A dot over a symbol indicates the first derivative with respect to time.

INTRODUCTION

A robot arm should obey movement commands from an operator or computer program as closely as possible. Singularities in the mathematical equations that translate these commands into arm movements hinder this objective. One solution is simply to avoid the singular position of the robot arm that causes a singularity (refs. 1 and 2). However, in using resolved-rate equations (ref. 3), an operator generally issues commands to the robot hand, and to move the hand as commanded, the arm may inadvertently pass through a singularity. Erratic motion may result until the arm moves sufficiently far from the singularity. A better solution appears to be the use of a different set of equations at or near singularities (ref. 4). Of course, the transition from one set of equations to the other should produce the overall motion that an operator wants.

This paper discusses the kinematic equations of motion for a six-degree-of-freedom manipulator with which the hand is positioned (translated) by three rotational joints (waist, shoulder, and elbow) and oriented by three additional rotational joints (wrist). When the elbow joint angle is zero, the robot arm is fully extended (straightened) and the regular resolved-rate equations (refs. 4 and 5, for example) become singular (division by zero). This paper presents equations which can be used, instead of the regular resolved-rate equations, to translate the robot hand in the neighborhood of the singularity. These equations are demonstrated in a kinematic simulation of a robot arm with the same geometric parameters assumed in reference 4. As the robot arm is being fully extended to the singular elbow position, motions (joint angles and joint angle rates) are compared for these equations and the regular resolved-rate equations. Finally, two integration methods (Euler and Adams-Bashforth second-order predictor integration methods) are compared for three integration step sizes.

ANALYSIS

A robot arm and its joint axis systems are illustrated in figure 1. Similar arms are used in manufacturing by moving the arm through a sequence of prerecorded joint angles. Another method of control is teleoperation, where an operator can command either joint angle rates or translation rates and rotation rates with respect to some axis system, and then a computer resolves the commands into appropriate joint angle rates ($\dot{\theta}_i$, $i = 1, 2, \ldots, 6$). A simplifying assumption is that wrist rotation does not translate the robot hand axis system.

Operator translational velocity commands in the hand axis system are tranformed to the base axis system by

$$\vec{V}_0 = \mathbf{L}\,\vec{V}_6 \tag{1}$$

where $\mathbf{L}$ is a transformation matrix (appendix A). The waist, shoulder, and elbow joint rates then satisfy the equation

$$\vec{V}_0 = \mathbf{J}_1 \begin{pmatrix} \dot{\theta}_1 \\ \dot{\theta}_2 \\ \dot{\theta}_3 \end{pmatrix} \tag{2}$$

where $\mathbf{J}_1$ is an appropriate Jacobian matrix (appendix A).

The inverse of equation (2) is

$$\begin{pmatrix} \dot{\theta}_1 \\ \dot{\theta}_2 \\ \dot{\theta}_3 \end{pmatrix} = \mathbf{J}_1^{-1} \begin{pmatrix} V_{XO} \\ V_{YO} \\ V_{ZO} \end{pmatrix} \tag{3}$$

provided the inverse matrix $\mathbf{J}_1^{-1}$ exists. Equation (3) is the translational part of the resolved-rate equations that gives the joint rates necessary to move the robot hand axis system as commanded by an operator.

The determinant of $\mathbf{J}_1$ is (appendix A)

$$\det(\mathbf{J}_1) = [\sin\theta_2 + \sin(\theta_2 + \theta_3)]\sin\theta_3 \, \imath_{ES}^3 \tag{4}$$

Singularities occur whenever this determinant is zero. Since $\imath_{ES} \neq 0$, the singular conditions are:

$$\sin\theta_3 = 0 \tag{5}$$

$$\sin\theta_2 + \sin(\theta_2 + \theta_3) = 0 \tag{6}$$

In equation (5), $\theta_3 = 0°$, which means that the robot arm is at its maximum extension. ($\theta_3 = \pm 180°$ is not achievable with the robot arm in fig. 1. See table I for geometric parameters of the robot arm.) Equation (6) means that the robot wrist is at its minimum distance ($\imath_{SN}$) from the line of rotation of the waist joint.

Analysis and simulation were conducted to develop techniques to maintain resolved-rate control in the vicinity of (or at) the singularity. Subsequent sections describe the method that was developed. The equations presented are used in the vicinity of the singularity and allow continued translation control. Outside of the singular region the regular resolved-rate equations (appendix A) are applicable.

Robot Arm Movement To Handle Elbow Joint Singularity

The singular position of the robot arm is illustrated in figure 2(a). To retract the robot hand, the elbow (θ_3) must bend either positively (fig. 2(b)) or negatively. Simultaneously, the shoulder joint (θ_2) moves in the opposite direction to keep the robot hand moving along the dashed straight line passing through the shoulder and wrist of the robot arm (points S and W in figs. 1 and 2).

V_T, V_P, and V_R rates.- The operator's translational control inputs are resolved into the velocity components shown in figure 2(b). The velocity component V_T lies along the dashed line from the shoulder to the wrist; V_P is perpendicular to the dashed line and, with respect to figure 1, is parallel to Y_2; V_R is parallel to Z_2 in figure 1 and completes a right-hand coordinate system with V_T and V_P. Movement of the robot arm is based on these rates. The arm pitches ($\dot{\theta}_2$) in proportion to V_P, rotates ($\dot{\theta}_1$) in proportion to V_R, and extends ($\dot{\theta}_3$) in proportion to V_T. An additional function of the shoulder joint ($\dot{\theta}_2$) is to null any movement of the robot hand off the dashed line which is caused by retraction or extension ($\dot{\theta}_3$). Expressions for V_T, V_P, and V_R are in appendix B.

Elbow joint angle rate $\dot{\theta}_3$.- The table inset in figure 3 indicates the direction of $\dot{\theta}_3$ for the different signs on θ_3 and V_T. For example, if θ_3 is positive and V_T is positive, then $\dot{\theta}_3$ must be negative to move the robot hand outward. Notice that the sign of $\dot{\theta}_3$ is opposite to the product of V_T and the sign of θ_3. The joint angle rate is made proportional to V_T as

$$\dot{\theta}_3 = -K_3 V_T \operatorname{sgn} \theta_3 \tag{7}$$

where K_3 is a specified constant, which is assumed to be unity in this paper.

A region about the elbow joint singularity is defined as

$$|\theta_3| < \delta_3 \tag{8}$$

where δ_3 is an assigned constant. Whenever the condition in equation (8) is detected, equation (7) is applied until the sign of θ_3 changes, which means θ_3 passes through 0° and is approximately 0°. The arm holds this extension (but is still free to move in pitch and yaw) until a negative V_T is commanded to retract the arm. This is better explained later in a flow diagram for the translational equations.

If the maximum absolute value of $\dot{\theta}_3$ is M and if the integration step size is h, then δ_3 in equation (8) should exceed

$$\delta_{min} = Mh \tag{9}$$

Thus, for $h = 1/32$ sec and $M = 0.5$ rad/sec, $\delta_{min} = 0.895°$ or 0.0156 rad. For test applications in this paper, δ_3 was chosen as 1°.

Shoulder joint angle rate $\dot{\theta}_2$.- The joint angle rate $\dot{\theta}_2$ is the sum of two other rates: $\dot{\sigma}$ and $\dot{\rho}$. The $\dot{\sigma}$ component coordinates with $\dot{\theta}_3$ to keep the robot hand on the dashed line in figure 4. The component $\dot{\rho}$ accounts for a pitching command from an operator.

First, consider the rate $\dot{\sigma}$. By the law of cosines

$$l_{WS}^2 = l_{ES}^2 + l_{WE}^2 + 2 l_{ES} l_{WE} \cos \theta_3 \tag{10}$$

where l_{WS} is the distance between the wrist and shoulder (points W and S in fig. 1). Differentiating equation (10),

$$l_{WS} \dot{l}_{WS} = -l_{ES} l_{WE} (\sin \theta_3) \dot{\theta}_3 \tag{11}$$

By the law of sines,

$$\sin \sigma = \frac{-l_{WE} \sin \theta_3}{l_{WS}} \tag{12}$$

By the law of cosines,

$$\cos \sigma = \frac{l_{ES}^2 + l_{WS}^2 - l_{WE}^2}{2 l_{ES} l_{WS}} \tag{13}$$

Differentiate equation (12) to obtain

$$\dot{\sigma} = \frac{-l_{WE}}{\cos \sigma} \frac{l_{WS} (\cos \theta_3) \dot{\theta}_3 - (\sin \theta_3) \dot{l}_{WS}}{l_{WS}^2} \tag{14}$$

With equations (11) and (13), equation (14) is

$$\dot{\sigma} = \frac{-2\ell_{WE}\ell_{ES}}{\ell_{ES}^2 + \ell_{WS}^2 - \ell_{WE}^2}\left(\cos\theta_3 + \frac{\ell_{ES}\ell_{WE}\sin^2\theta_3}{\ell_{WS}^2}\right)\dot{\theta}_3 \tag{15}$$

Second, consider the rate $\dot{\rho}$ to pitch the robot arm in response to an operator's command. The robot wrist has a moment arm ℓ_{WS} relative to the shoulder of the robot arm. Hence, the linear pitching rate V_p is the product of this moment arm and the angular pitch rate $\dot{\rho}$ so that

$$\dot{\rho} = \frac{V_p}{\ell_{WS}}$$

where

$$\ell_{WS} = \sqrt{\ell_{ES}^2 + \ell_{WE}^2 + 2\ell_{ES}\ell_{WE}\cos\theta_3} \tag{16}$$

In this paper, $\ell_{ES} = \ell_{WE}$, and the pertinent equations to compute the shoulder joint angle rate $\dot{\theta}_2$ are as follows:

$$\dot{\sigma} = \frac{-\dot{\theta}_3}{2} \tag{17}$$

$$\ell_{WS} = \ell_{ES}\sqrt{2(1 + \cos\theta_3)} \tag{18}$$

$$\dot{\rho} = \frac{V_p}{\ell_{WS}} \tag{19}$$

$$\dot{\theta}_2 = \dot{\sigma} + \dot{\rho} \tag{20}$$

Waist joint angle rate $\dot{\theta}_1$.- The component of the commanded translational velocity in the direction of Z_2 in figure 1 is (from eqs. (B6) and (B7))

$$V_R = -\sin \theta_1 \, V_{XO} + \cos \theta_1 \, V_{YO} \tag{21}$$

If the robot wrist (point W in fig. 1) projects onto the negative X_1-axis, a positive waist rotation ($\dot{\theta}_1$) is needed to cause a positive linear rate V_R along Z_2. But, if the wrist projects onto the positive X_1-axis, a negative $\dot{\theta}_1$ rotation is needed for a positive linear rate V_R along Z_2. The projection of the robot wrist position onto the X_1-axis is

$$P = -\sin(\theta_2 + \theta_3) \, \imath_{WE} - \sin \theta_2 \, \imath_{ES} \tag{22}$$

Therefore,

$$\dot{\theta}_1 = \frac{-V_R}{\ell} \operatorname{sgn} P \tag{23}$$

translates the robot wrist located at a distance (fig. 4)

$$\ell = \sqrt{\imath_{SN}^2 + P^2} \tag{24}$$

from the line of rotation of the waist joint with a linear rate V_R. The case of $\imath_{WE} = \imath_{ES}$ and $P = 0$ (that is, at the singularity $\sin \theta_2 + \sin(\theta_2 + \theta_3) = 0$ (eq. (4))) is considered later.

Logic flow for translational equations.- The logical flow for computing the joint angle rates $\dot{\theta}_1$, $\dot{\theta}_2$, and $\dot{\theta}_3$ is shown in figure 5. In the block diagram, an operator issues translational velocity commands to the robot hand. These commands are then transformed from the robot hand axis system (X_6, Y_6, Z_6) to the base axis system (X_0, Y_0, Z_0). If θ_3 does not fall within the singular region ($|\theta_3| < \delta_3$), the regular resolved-rate equations are used and θ_3^* is equated to θ_3 for later use. The resolved-rate equations yield joint angle rates which are integrated to get joint angles to drive the robot arm. The operator observes the resulting motion and issues new commands.

If θ_3 does fall within the singular region, the equations indicated in the dashed box (fig. 5) are used. As an example, suppose the robot arm is initially in position 1 in figure 6 and, in the next time increment, moves to position 2 where θ_3 is within the singular region. On the first pass through the dashed box, θ_3^* is positive (since θ_3 was positive at position 1) and the current θ_3 at position 2 is positive, so their product is positive. Thus, $\dot{\theta}_3$ is computed with equation (7)

and, for positive V_T, is negative. When θ_3 becomes negative in the singular region, the product of $\dot{\theta}_3^*$ and the current θ_3 is negative. Therefore, for positive V_T, no further change in θ_3 is allowed ($\dot{\theta}_3 = 0$). However, suppose a negative V_T is commanded. Since θ_3 is now negative and V_T is negative, $\dot{\theta}_3$ is negative (table in fig. 3), and the robot arm retracts by bending the elbow joint in a direction opposite to that with which it entered the singular region. If an elbow bend does not suit an operator, he simply straightens ($\theta_3 = 0°$) and retracts the robot arm again.

If the elbow of a robot arm is bent down (position 2 in fig. 6) and an operator commands negative V_T to retract the robot arm before it straightens, then the arm will maintain a downward bent elbow as it retracts.

In this study, an Adams-Bashforth second-order predictor integration method

$$\theta_i(k+1) = \frac{h}{2}\left[3\dot{\theta}_i(k) - \dot{\theta}_i(k-1)\right] + \theta_i(k) \tag{25}$$

is used with a nominal value of $h = 1/32$ sec to integrate the joint angle rates to get the joint angles. When θ_3 falls into the singular region, and the arm is fully extended with $V_T > 0$, $\dot{\theta}_3 = 0$ in figure 5. In figure 5, $\theta_{3,p}$ is then used to hold the current value of θ_3; this is required because equation (25) would compute a new θ_3, different from the current value, since the equation contains both present and past values of $\dot{\theta}_3$. If Euler integration

$$\theta_i(k+1) = h\dot{\theta}_i(k) + \theta_i(k) \tag{26}$$

is used, $\theta_{3,p}$ would not be required since only the current value of $\dot{\theta}_3$ appears in equation (26).

Pitching robot arm at full extension.- For discussion purposes, let the robot hand in figure 7 be oriented the same as that in figure 1. Then if an operator commands a pitch down with V_{X6}, the arm will pitch down according to equation (19). However, in this paper, the robot arm stops when θ_3 changes sign so that θ_3 is not exactly zero. Hence, in figure 7(b), when the operator attempts to pitch the arm down, there is a negative V_T, which causes the arm to retract as it pitches down. Pitching the arm up would not cause any retraction because the V_T rate would be positive. Since the arm is in the stopped extended position and $V_T > 0$, the arm will not retract.

To have the robot arm maintain its full extension (whether pitching up or down) until specifically commanded by an operator to retract, simply replace $V_T > 0$ in figure 5 with $V_{Z6} > 0$. The arm will then only retract from the stopped extended position if the operator commands a negative V_{Z6}.

Robot Arm Movement To Handle Wrist-Waist Singularity

With variations in θ_1 (fig. 1), the robot hand generates a circle about Z_0. Equation (6), or equivalently,

$$\theta_3 = -2\theta_2 \tag{27}$$

means that the minimum radius for this circular motion has been reached (fig. 8) and the resolved-rate equations are singular.

In this paper, when

$$|\sin \theta_2 + \sin(\theta_2 + \theta_3)| < \delta_{23} \tag{28}$$

where δ_{23} is chosen as 0.001 to prevent erratic motions at the singularity, equations (7), (20), and (23) are used. In equation (23), $\ell = \imath_{SN} \neq 0$ for the wrist-waist singularity.

Robot Arm Movement in Cylindrical-Type Coordinates

Thus far, the operator's translational velocity command to the robot hand has been $\vec{V}_6$, which is then resolved into joint angle rates in the robot arm. In the singular elbow region, $\vec{V}_6$ is resolved in directions of thrust, pitch, and rotate in figure 4 to obtain the rates V_T, V_P, and V_R, which are then used to move the robot arm according to equations (7), (20), and (23). As an alternate means of control, the operator can be given the option of directly specifying V_T, V_P, and V_R with his controller inputs. This mode does not constitute movement in true cylindrical coordinates because of the shoulder offset $\imath_{SN}$ from the waist station (fig. 4).

Inside the singular region $(|\theta_3| < \delta_3)$, $\dot{\theta}_3$ can be made proportional to V_T (eq. (7)); however, outside the singular region $(|\theta_3| > \delta_3)$, the robot hand should extend and retract along $\imath_{WS}$ in figure 4 with the actual commanded V_T rate. The appropriate equation for $\dot{\theta}_3$ follows immediately from equation (11) with the substitution

$$\dot{\imath}_{WS} = V_T \tag{29}$$

as

$$\dot{\theta}_3 = -\frac{\imath_{WS}}{\imath_{ES}\,\imath_{WE}} \frac{V_T}{\sin \theta_3} \tag{30}$$

Notice that the sign of $\dot{\theta}_3$ is consistent with the table in figure 3; that is, when V_T is positive and θ_3 is negative, $\dot{\theta}_3$ is positive.

RESULTS AND DISCUSSION

The kinematic equations for translation control, including the equations to be used in the singularity region, were programmed on a CDC® CYBER 175 computer operating in real time, interfaced to an ADAGE GPS/340 graphics system, and the manned control station in the Intelligent Systems Research Laboratory (ref. 6).

To command translational movements of the robot hand, an operator used a three-axis hand controller: one degree of freedom for each of the robot hand speeds V_{X6}, V_{Y6}, and V_{Z6}. For example, in figure 1, the robot hand axis system is (X_6, Y_6, Z_6), and the operator commanded the hand to move in the X_6-direction by moving the controller in the direction corresponding to V_{X6}.

Based on kinematic equations, a graphically simulated robot arm was driven in response to an operator's velocity inputs to the robot hand. The operator observed the movement on a monitor and issued new commands. This simulation was primarily to spot potential operational problems and debug the computer program prior to using a real industrial robot arm.

A simple simulation experiment was conducted to compare the following two sets of equations, which can be used to control the robot arm in translational movement:

1. Translational equations in the present paper (eqs. (A6) to (A12) in conjunction with eqs. (7), (20), and (23))

2. Regular resolved-rate equations (eqs. (A6) to (A12))

Variations in the joint angles θ_2 and θ_3 and the joint angle rates $\dot{\theta}_2$ and $\dot{\theta}_3$ were compared for both extension and retraction movements of the robot arm.

A second simulation experiment was conducted with the translational equations in the present paper to evaluate the effects of two different numerical integration techniques (Adams-Bashforth second-order predictor and Euler), three different integration step sizes (1/16, 1/32, and 1/64 sec), and combinations of the numerical integration techniques and step sizes.

Simulated Arm Movement Through Elbow Singular Region

The robot arm was initially positioned for the extension maneuver with the joint angle values $\theta_2 = -30°$ and $\theta_3 = -60°$. Then, with a switch located on a real-time control console, a computer operator issued a translational velocity command $V_{Z6} = 40$ mm/sec to extend the robot arm.

The variations in joint angles θ_2 and θ_3 and their rates $\dot{\theta}_2$ and $\dot{\theta}_3$ for both control algorithms are plotted in figures 9 and 10 against time.

Equations in present paper.- With respect to the elbow joint singularity ($\theta_3 = 0°$), the equations developed in the present paper are used when θ_3 is within $\pm 1°$ of full arm extension ($\theta_3 = 0°$); that is, $\delta_3 = 1°$ in equation (8). In

figure 10, the final zero joint rates $\dot{\theta}_2 = 0$ and $\dot{\theta}_3 = 0$ stop the robot arm in the extended position ($\theta_3 = 0°$ and $\theta_2 = -63°$ in fig. 9). Although the robot arm is fully extended, the operator maintains the input command $V_{Z6} = 40$ mm/sec, which causes θ_2 in figure 9 to increase slightly with time. The reason for this continued variation is that the arm stops extending at a small positive value of θ_3 (the value depends on the integration step size). With the robot hand oriented with respect to the forearm as shown in figure 1, a small positive θ_3 with $V_{Z6} = 40$ mm/sec produces a small pitch-down component (positive V_p). By equations (19) and (20), $\dot{\theta}_2$ increases with V_p. This small variation is not anticipated to be a problem. By visual observation, the operator can issue commands to nullify any significant variations. Alternate approaches are to replace $V_T > 0$ with $V_{Z6} > 0$ in figure 5, or switch to cylindrical-type coordinates while the robot arm is fully extended.

Resolved-rate equations.- After 3.5 sec in figure 10, the regular resolved-rate equations produce undesirable high frequency oscillations in $\dot{\theta}_2$ and $\dot{\theta}_3$. The oscillation for $\dot{\theta}_3$ lies between the upper and lower limits of joint angle rate of ±28.6 deg/sec. The oscillation in $\dot{\theta}_2$ is half that in $\dot{\theta}_3$ (eq. (17)) or approximately ±15 deg/sec. These oscillations totally obscure the region between the oscillation boundaries. The joint angles θ_2 and θ_3 in figure 9 also show high frequency oscillations with amplitudes of about 1°.

For the retraction maneuver, the robot arm was initially positioned with joint angle values of $\theta_2 = -60°$ and $\theta_3 = 0°$ for both the regular resolved-rate equations and the equations of the present paper. As with the extension maneuver, a switch was used to issue a negative translational velocity command V_{Z6} to retract the robot arm. No differences in joint angles or their rates were seen between the two control algorithms.

Comparisons of Integration Schemes and Step Sizes

The nominal integration scheme and step size used in the present paper are Adams-Bashforth second-order predictor and 1/32 sec, respectively. The question arose as to whether a simpler integration scheme and/or a different step size would have any effect on the system as defined for this study. The reason for this question was that another user might be constrained by computer capacities especially if real-time operation were required. Runs were conducted by using the translational control algorithms of the present paper to answer these questions.

Comparisons are presented in figure 11 of joint angle movements and joint angle rates determined by using, first, the Adams-Bashforth second-order predictor scheme and, then, the simpler Euler scheme for the extension maneuver. The step size for both calculations was 1/32 sec. The only difference seen between the two schemes occurs at the end of the extension maneuver. This difference appears to be caused by the arm extending to slightly different positions (θ_3) because of the differences in the integration schemes. Thus, the user could take advantage of the simpler Euler integration scheme.

To look at the effect of step size, the simpler Euler integration scheme was chosen for presentation in the present paper, since with the Adams-Bashforth scheme, no meaningful differences were observed. Comparisons with different step sizes, 1/16, 1/32, and 1/64 sec, are presented in figure 12. Little or no differences exist

between 1/32 and 1/64 sec. The difference which occurs for 1/16 sec in the extension maneuver is caused by the deadband around θ_3. One other difference which occurs at the end of the extension maneuver for the step size of 1/16 sec is the slightly exaggerated effect caused by the small pitch (θ_2) component which exists when θ_3 is not exactly zero as was discussed earlier in this paper (fig. 7). It appears that a user could take advantage of using the Euler integration scheme and a step size of 1/16 sec when using the system modelled in this paper. It is advisable, however, for the user to examine his situation carefully before making this decision.

CONCLUDING REMARKS

An operator commands the robot hand to move in a certain direction by commanding a velocity in that direction. Resolved-rate equations relate the operator's commands to joint angle rates in the robot arm to move the hand. However, when the arm is fully extended, the equations become singular in the elbow joint variable. The present paper has presented a set of equations that enable control of the robot arm within the singular region.

The resolved-rate equations are used, except when the elbow joint angle falls within a specified region (which includes the singular position). In this region, the commanded translational velocity is resolved relative to a straight line passing through the shoulder and wrist of the robot arm. The elbow joint angle rate is then made proportional to the component lying along the line. The shoulder joint moves in the opposite direction to that of the elbow so that the hand retracts and extends along this line. Also, within this region, the shoulder joint pitches the robot arm in response to pitch command, and the waist joint rotates the robot arm about its base.

The equations in this paper give the operator the option to bend the robot arm at the elbow in either the up or down direction. The operator simply extends the arm and backs it up again to automatically reverse the direction of the elbow bend.

The equations which handle the elbow joint singularity and the equations which allow cylindrical-type movement of the robot arm were applied to move a graphically simulated robot arm. The desired motions were obtained, and the equations will be used in other experimental tests.

At the elbow joint singularity, undesirable joint rate oscillations result from an implementation of the regular resolved-rate equations but not in the translational equations presented in the present paper.

Finally, a simple experiment was conducted to compare two integration methods (Adams-Bashforth second-order predictor and Euler) and three integration step sizes (1/16, 1/32, and 1/64 sec). There were little or no differences seen in either set of tests. Therefore, it appears that if a user is constrained in the area of computer power, the simpler Euler integration scheme with a step size of 1/16 sec can be

used. However, it is advisable for the user to examine the situation carefully before making a decision.

Langley Research Center
National Aeronautics and Space Administration
Hampton, VA 23665
September 19, 1984

APPENDIX A

MATRICES $\mathbf{L}$ and $\mathbf{J}_1$

With respect to the robot hand axis system, an operator commands the translational velocity $\vec{V}_6$, which is then transformed to the base coordinate system by

$$\vec{V}_0 = \mathbf{L}\,\vec{V}_6 \tag{A1}$$

With the robot arm parameters in reference 4 (table I), the equations to compute the elements of the transformation matrix $\mathbf{L}$ in reference 5 become

$$\left.\begin{aligned}
Q_1 &= \cos\theta_4 \cos\theta_5 \cos\theta_6 - \sin\theta_4 \sin\theta_6 \\
Q_2 &= \sin\theta_4 \cos\theta_5 \cos\theta_6 + \cos\theta_4 \sin\theta_6 \\
Q_3 &= -\cos\theta_4 \cos\theta_5 \sin\theta_6 - \sin\theta_4 \cos\theta_6 \\
Q_4 &= -\sin\theta_4 \cos\theta_5 \sin\theta_6 + \cos\theta_4 \cos\theta_6 \\
P_1 &= -\cos(\theta_2 + \theta_3) \\
P_2 &= -\sin(\theta_2 + \theta_3) \qquad \text{(This represents a correction to ref. 5.)} \\
\\
T_1 &= -\sin\theta_1 \\
T_2 &= -\cos\theta_1\, P_2 \\
T_3 &= \cos\theta_1 \\
T_4 &= -\sin\theta_1\, P_2 \\
\\
L_{11} &= -\cos\theta_1\, P_1 Q_1 + T_1 Q_2 - T_2 \sin\theta_5 \cos\theta_6 \\
L_{21} &= -\sin\theta_1\, P_1 Q_1 + T_3 Q_2 - T_4 \sin\theta_5 \cos\theta_6 \\
L_{31} &= P_2 Q_1 + P_1 \sin\theta_5 \cos\theta_6 \\
\\
L_{12} &= -\cos\theta_1\, P_1 Q_3 + T_1 Q_4 + T_2 \sin\theta_5 \sin\theta_6 \\
L_{22} &= -\sin\theta_1\, P_1 Q_3 + T_3 Q_4 + T_4 \sin\theta_5 \sin\theta_6 \\
L_{32} &= P_2 Q_3 - P_1 \sin\theta_5 \sin\theta_6 \\
\\
L_{13} &= -\cos\theta_1\, P_1 \cos\theta_4 \sin\theta_5 + T_1 \sin\theta_4 \sin\theta_5 + T_2 \cos\theta_5 \\
L_{23} &= -\sin\theta_1\, P_1 \cos\theta_4 \sin\theta_5 + T_3 \sin\theta_4 \sin\theta_5 + T_4 \cos\theta_5 \\
L_{33} &= P_2 \cos\theta_4 \sin\theta_5 - P_1 \cos\theta_5
\end{aligned}\right\} \tag{A2}$$

Rotations about the waist, shoulder, and elbow move the robot hand. This relationship is expressed as

$$\vec{V}_0 = \mathbf{J}_1 \begin{pmatrix} \dot{\theta}_1 \\ \dot{\theta}_2 \\ \dot{\theta}_3 \end{pmatrix} \tag{A3}$$

where $\mathbf{J}_1$ (from ref. 4) is (assume $\iota_{ES} = \iota_{WE}$)

$$\mathbf{J}_1 = \begin{bmatrix} -\sin\theta_1[\sin\theta_2 + \sin(\theta_2+\theta_3)]\iota_{ES} - \cos\theta_1\,\iota_{SN} & \cos\theta_1[\cos\theta_2 + \cos(\theta_2+\theta_3)]\iota_{ES} & \cos\theta_1\cos(\theta_2+\theta_3)\,\iota_{ES} \\ \cos\theta_1[\sin\theta_2 + \sin(\theta_2+\theta_3)]\iota_{ES} - \sin\theta_1\,\iota_{SN} & \sin\theta_1[\cos\theta_2 + \cos(\theta_2+\theta_3)]\iota_{ES} & \sin\theta_1\cos(\theta_2+\theta_3)\,\iota_{ES} \\ 0 & -[\sin\theta_2 + \sin(\theta_2+\theta_3)]\iota_{ES} & -\sin(\theta_2+\theta_3)\,\iota_{ES} \end{bmatrix} \tag{A4}$$

The determinant of $\mathbf{J}_1$ is

$$\det(\mathbf{J}_1) = [\sin\theta_2 + \sin(\theta_2+\theta_3)]\sin\theta_3\,\iota_{ES}^3 \tag{A5}$$

Equation (A3) can be solved for the joint angle rates as follows:

$$\dot{\theta}_1 = \frac{(V_{X0}\sin\theta_1 - V_{Y0}\cos\theta_1)b_1\iota_{ES}^2}{\det(\mathbf{J}_1)} \tag{A6}$$

$$\dot{\theta}_2 = \frac{(V_{X0}b_2 + V_{Y0}b_3)\sin(\theta_2+\theta_3)\,\iota_{ES} + V_{Z0}[\sin\theta_2 + \sin(\theta_2+\theta_3)]\cos(\theta_2+\theta_3)\,\iota_{ES}^2}{\det(\mathbf{J}_1)} \tag{A7}$$

$$\dot{\theta}_3 = \frac{\{-V_{X0}b_2 + V_{Y0}b_3 + V_{Z0}[\cos\theta_2 + \cos(\theta_2+\theta_3)\,\iota_{ES}]\}\,[\sin\theta_2 + \sin(\theta_2+\theta_3)]\iota_{ES}}{\det(\mathbf{J}_1)} \tag{A8}$$

where

$$b_1 = \sin\theta_2\cos(\theta_2+\theta_3) - \cos\theta_2\sin(\theta_2+\theta_3) = -\sin\theta_3 \tag{A9}$$

$$b_2 = \cos\theta_2[\sin\theta_2 + \sin(\theta_2+\theta_3)]\iota_{ES} - \sin\theta_1\,\iota_{SN} \tag{A10}$$

$$b_3 = \sin\theta_1[\sin\theta_2 + \sin(\theta_2+\theta_3)]\iota_{ES} + \cos\theta_1\,\iota_{SN} \tag{A11}$$

The only problem with these equations occurs when $\det(\mathbf{J}_1) = 0$. In this paper, $\det(\mathbf{J}_1)$ is replaced by

$$\det(\mathbf{J}_1) = 10^{-5} \operatorname{sgn}[\det(\mathbf{J}_1)] \tag{A12}$$

whenever $|\det(\mathbf{J}_1)| < 10^{-5}$ to circumvent computational problems. The sign of $\det(\mathbf{J}_1)$ is considered positive when $\det(\mathbf{J}_1) = 0$. This paper presents a set of translational equations which are not affected by this condition.

APPENDIX B

THRUST, PITCH, AND ROTATE VELOCITY COMPONENTS OF ROBOT HAND

Components of the commanded translational velocity $\vec{V}_6$ of the robot hand (fig. 1) are related to its components in the axis system (X_2,Y_2,Z_2) as (ref. 5)

$$\begin{bmatrix} V_{X2} \\ V_{Y2} \\ V_{Z2} \end{bmatrix} = R_2^1 \, R_1^0 \begin{bmatrix} V_{X0} \\ V_{Y0} \\ V_{Z0} \end{bmatrix} \tag{B1}$$

where

$$R_2^1 = \begin{bmatrix} -\sin\theta_2 & \cos\theta_2 & 0 \\ -\cos\theta_2 & -\sin\theta_2 & 0 \\ 0 & 0 & 1 \end{bmatrix} \tag{B2}$$

$$R_1^0 = \begin{bmatrix} -\cos\theta_1 & -\sin\theta_1 & 0 \\ 0 & 0 & 1 \\ -\sin\theta_1 & \cos\theta_1 & 0 \end{bmatrix} \tag{B3}$$

$$V_{X2} = \sin\theta_2(\cos\theta_1 \, V_{X0} + \sin\theta_1 \, V_{Y0}) + \cos\theta_2 \, V_{Z0} \tag{B4}$$

$$V_{Y2} = \cos\theta_2(\cos\theta_1 \, V_{X0} + \sin\theta_1 \, V_{Y0}) - \sin\theta_2 \, V_{Z0} \tag{B5}$$

$$V_{Z2} = -\sin\theta_1 \, V_{X0} + \cos\theta_1 \, V_{Y0} \tag{B6}$$

Equations (B4) and (B5) represent corrections to reference 5.

The axis system (X_2,Y_2,Z_2) does not move with the forearm link (ι_{WE}). The velocity components V_T, V_P, and V_R indicated in figure 4 are given by

$$\begin{bmatrix} V_T \\ V_P \\ V_R \end{bmatrix} = \begin{bmatrix} \cos\sigma & -\sin\sigma & 0 \\ \sin\sigma & \cos\sigma & 0 \\ 0 & 0 & 1 \end{bmatrix} \begin{bmatrix} V_{X2} \\ V_{Y2} \\ V_{Z2} \end{bmatrix} \tag{B7}$$

REFERENCES

1. Klein, Charles A.; and Patterson, Mark R.: Computer Coordination of Limb Motion for Locomotion of a Multiple-Armed Robot for Space Assembly. IEEE Trans. Syst., Man, & Cybern., vol. SMC-12, no. 6, Nov./Dec. 1982, pp. 913-919.

2. Paul, Richard P.; and Stevenson, Charles N.: Kinematics of Robot Wrists. Int. J. Robotics Res., vol. 2, no. 1, Spring 1983, pp. 31-38.

3. Whitney, Daniel E.: Resolved Motion Rate Control of Manipulators and Human Prostheses. IEEE Trans. Man-Mach. Syst., vol. MMS-10, no. 2, June 1969, pp. 47-53.

4. Yeh, Shao-Chi: Locomotion of a Three-Legged Robot Over Structural Beams. M.S. Thesis, The Ohio State Univ., Aug. 1981.

5. Barker, L. Keith: Kinematic Equations for Resolved-Rate Control of an Industrial Robot Arm. NASA TM-85685, 1983.

6. Pennington, Jack E.: A Rate-Controlled Teleoperator Task With Simulated Transport Delays. NASA TM-85653, 1983.

TABLE I.- HOMOGENEOUS TRANSFORMATION MATRIX PARAMETERS

[From ref. 4]

Joint, i	α_i, deg	a_i, in.	r_i, in.	θ_i', deg	θ_i limits, deg
1	90	0	$*l_{NO}$	$\theta_1 + 180$	+160
2	0	$\S l_{ES}$	$\dagger l_{SN}$	$\theta_2 + 90$	+165
3	90	0	0	$\theta_3 + 90$	+135
4	90	0	$\ddagger l_{WE}$	$\theta_4 + 180$	+135
5	90	0	0	$\theta_5 + 180$	+105
6	0	0	$\# l_{HW}$	θ_6	+270

$*l_{NO}$ = Length from neck to base = 26 in. (66.05 cm)

$\S l_{ES}$ = Length from elbow to shoulder = 17 in. (43.18 cm)

$\dagger l_{SN}$ = Length from shoulder to neck = 6 in. (15.24 cm)

$\ddagger l_{WE}$ = Length from wrist to elbow = 17 in. (43.18 cm)

$\# l_{HW}$ = Length from hand to wrist = 6 in. (15.24 cm)

(In kinematic equations, distance from hand axis system to wrist is assumed to be 0.)

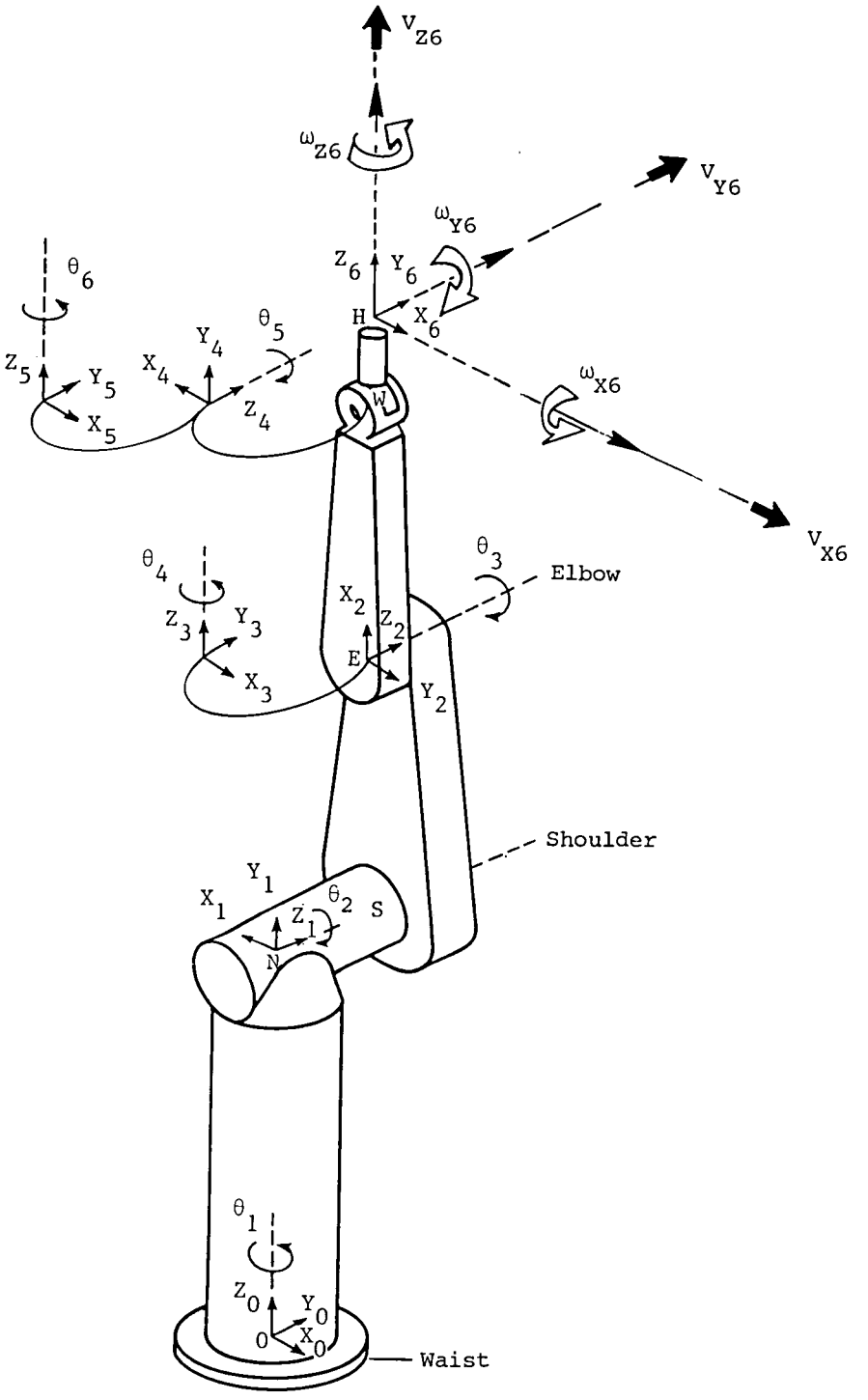

Figure 1.- Initial position of robot arm, joint axis systems, and commanded robot hand velocities.

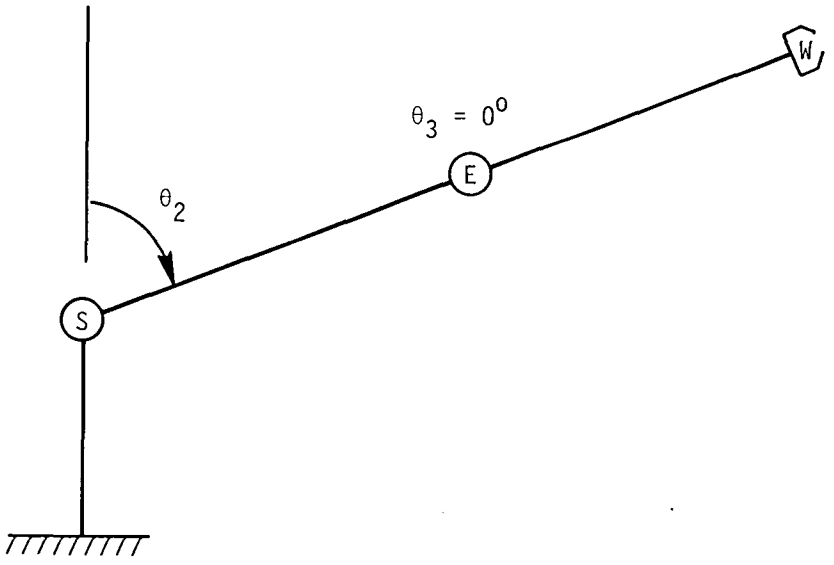

(a) Fully extended robot arm.

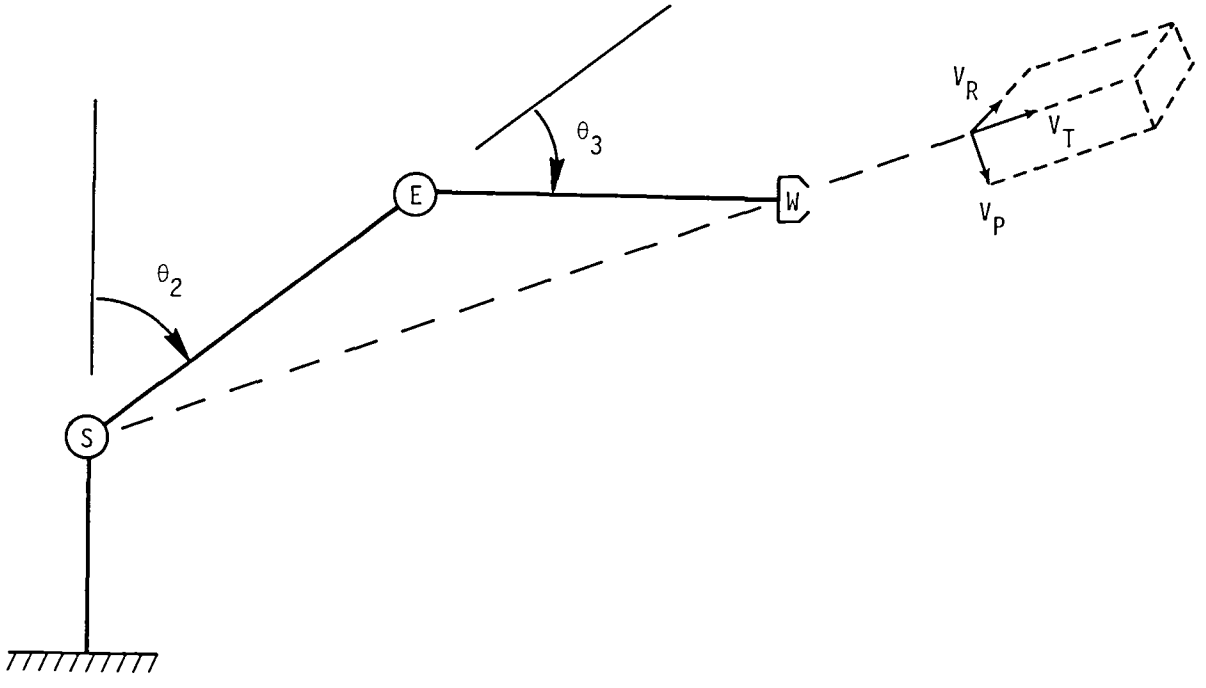

(b) Velocity components.

Figure 2.- Straightened robot arm (singular elbow position) and velocity components used to move arm near or at this position.

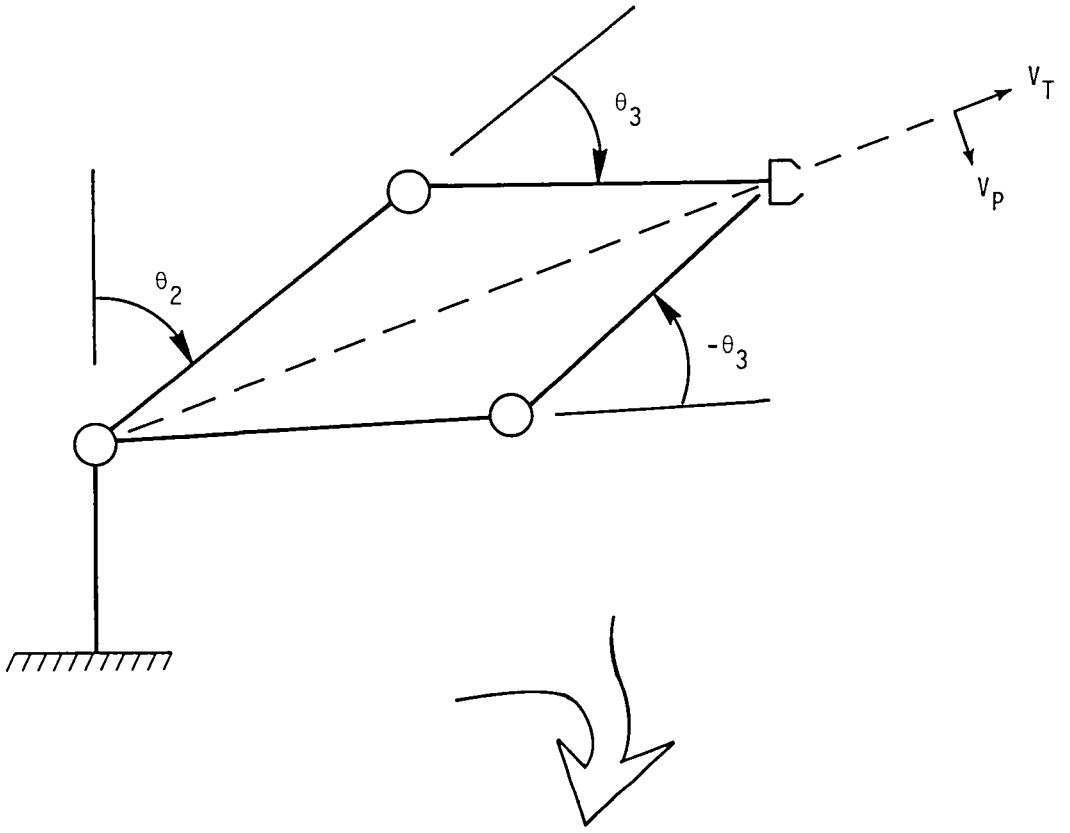

Algebraic sign on -		
θ_3	V_T	$\dot{\theta}_3$
+	+	-
+	-	+
-	+	+
-	-	-

Figure 3.- Retracting and extending robot arm.

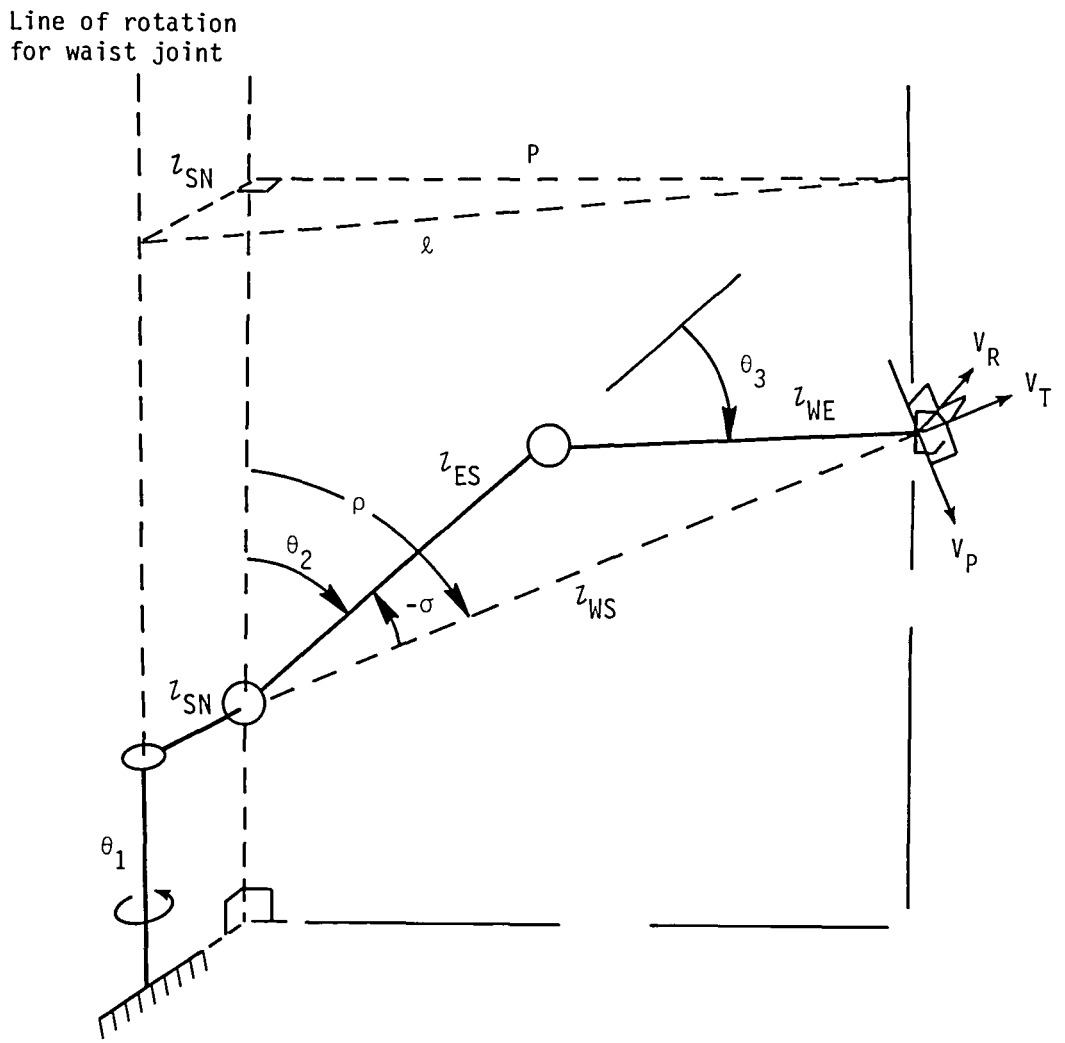

Figure 4.- Geometry used to derive joint speeds for shoulder and waist.

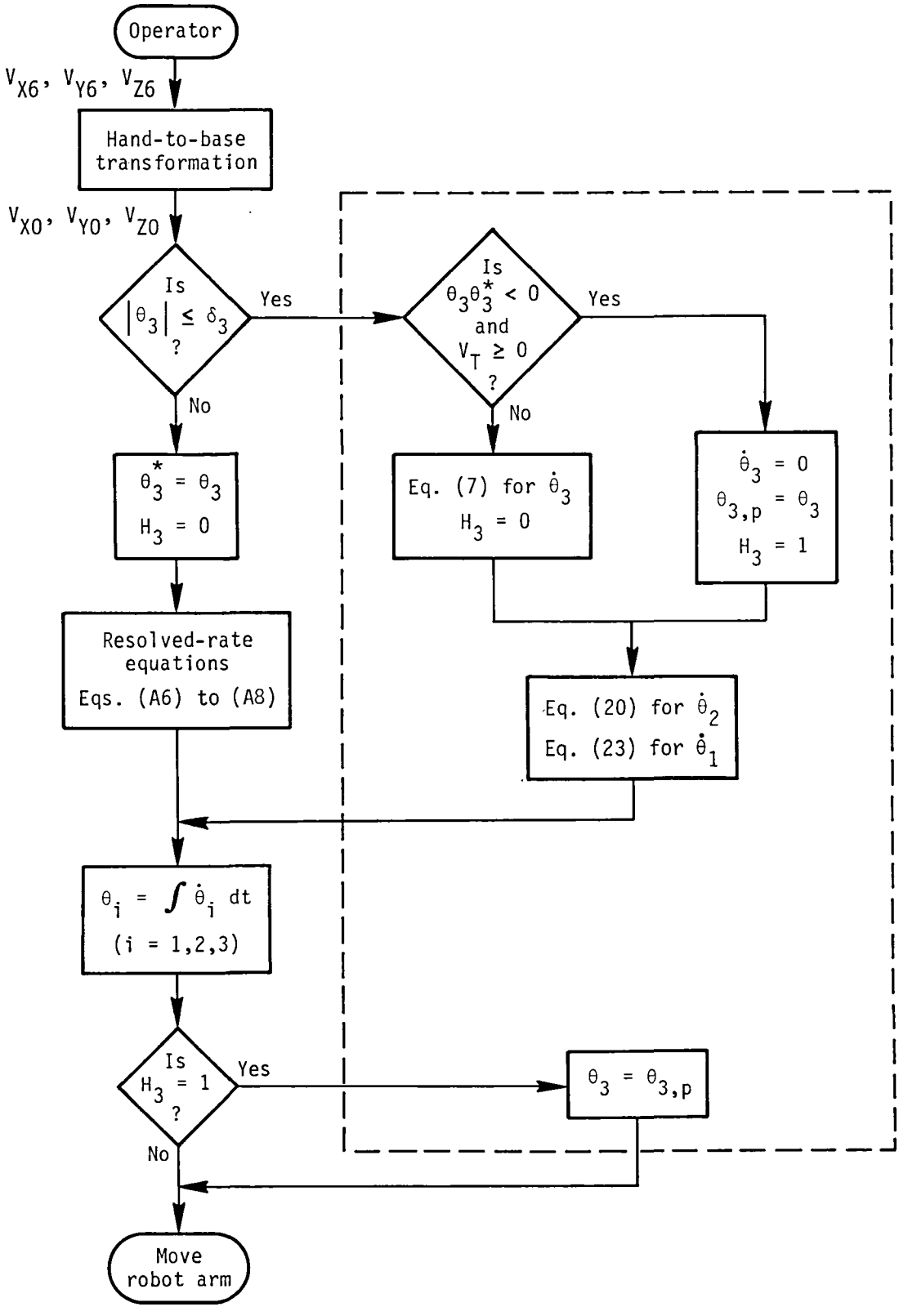

Figure 5.- Block diagram indicating implementation of logic flow for translational equations to move robot arm.

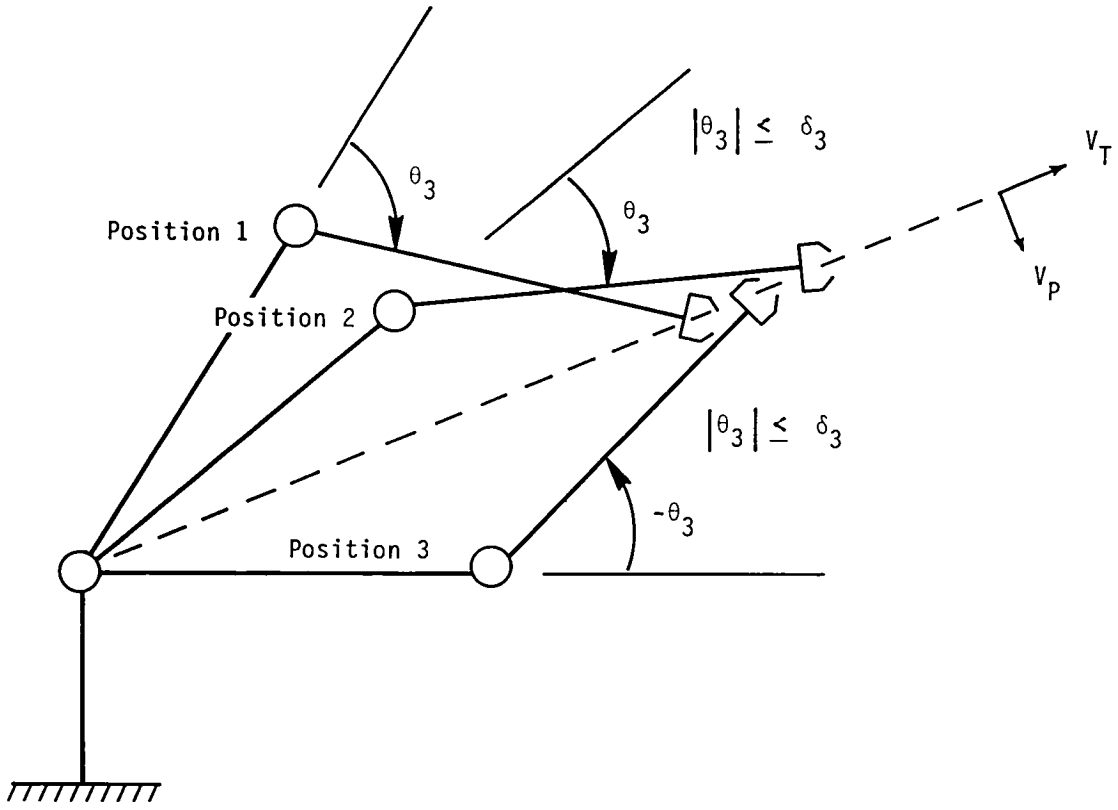

Figure 6.- Drawing used to describe motion of robot arm in singular elbow region.

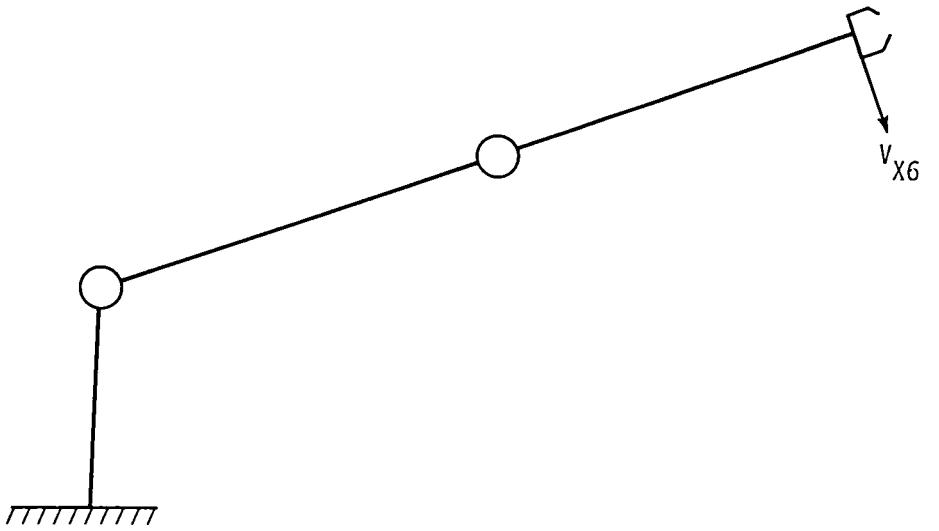

(a) Zero elbow joint angle.

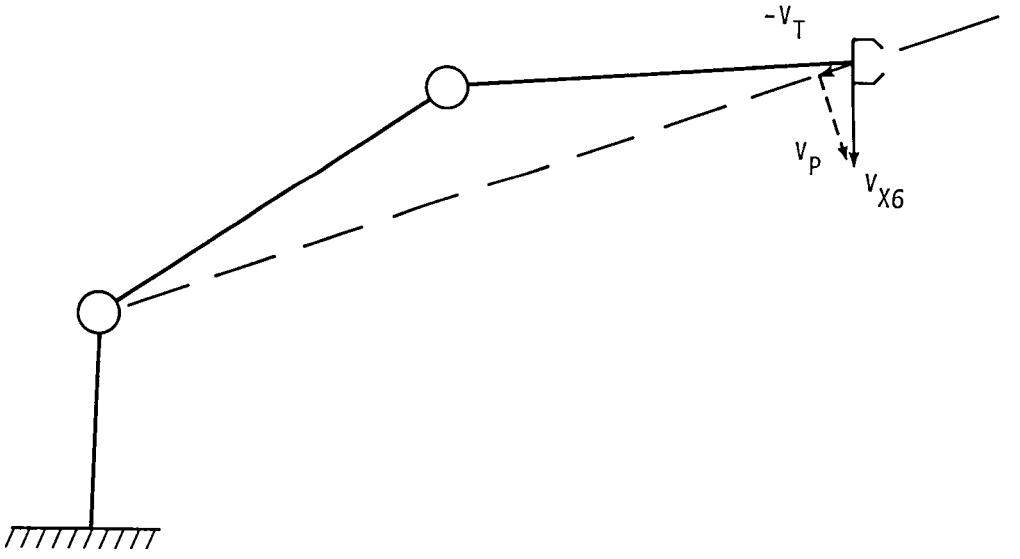

(b) Small nonzero elbow joint angle when further extension of robot arm is stopped.

Figure 7.- Drawing to indicate pitching motion of robot arm.

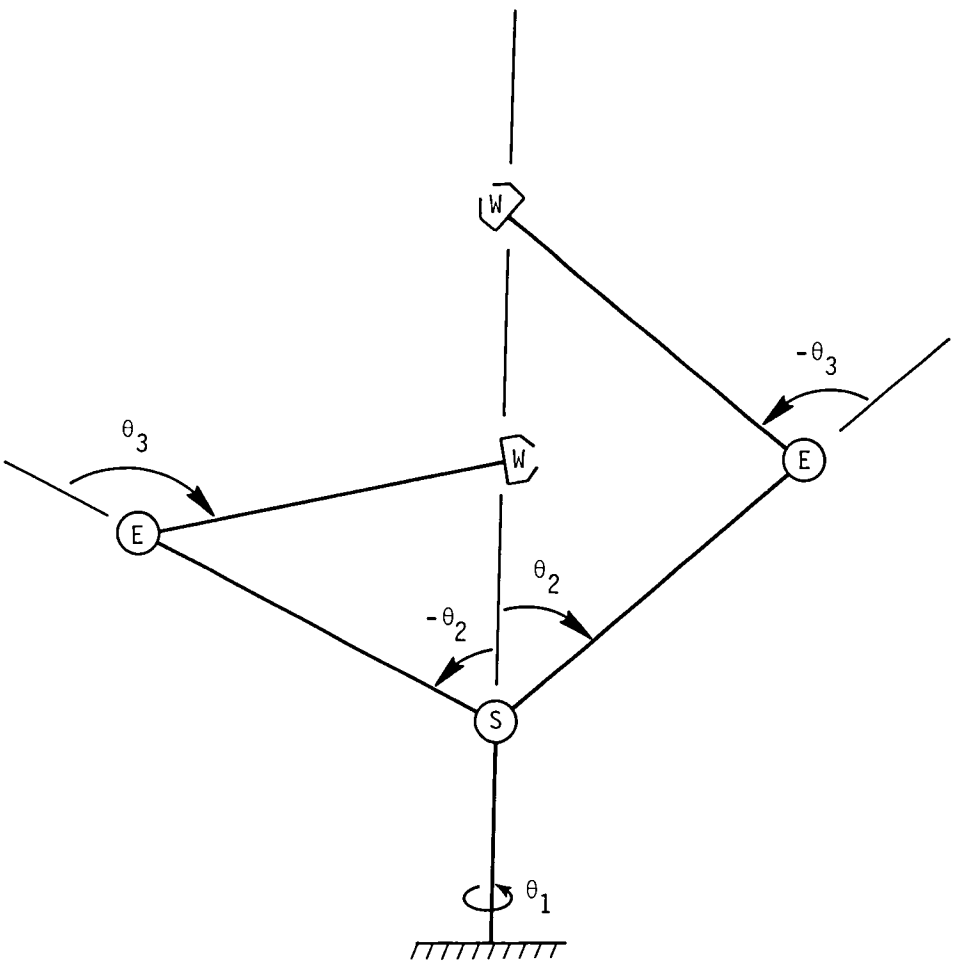

Figure 8.- Diagram to illustrate positions of robot arm at wrist-waist singularity in resolved-rate equations.

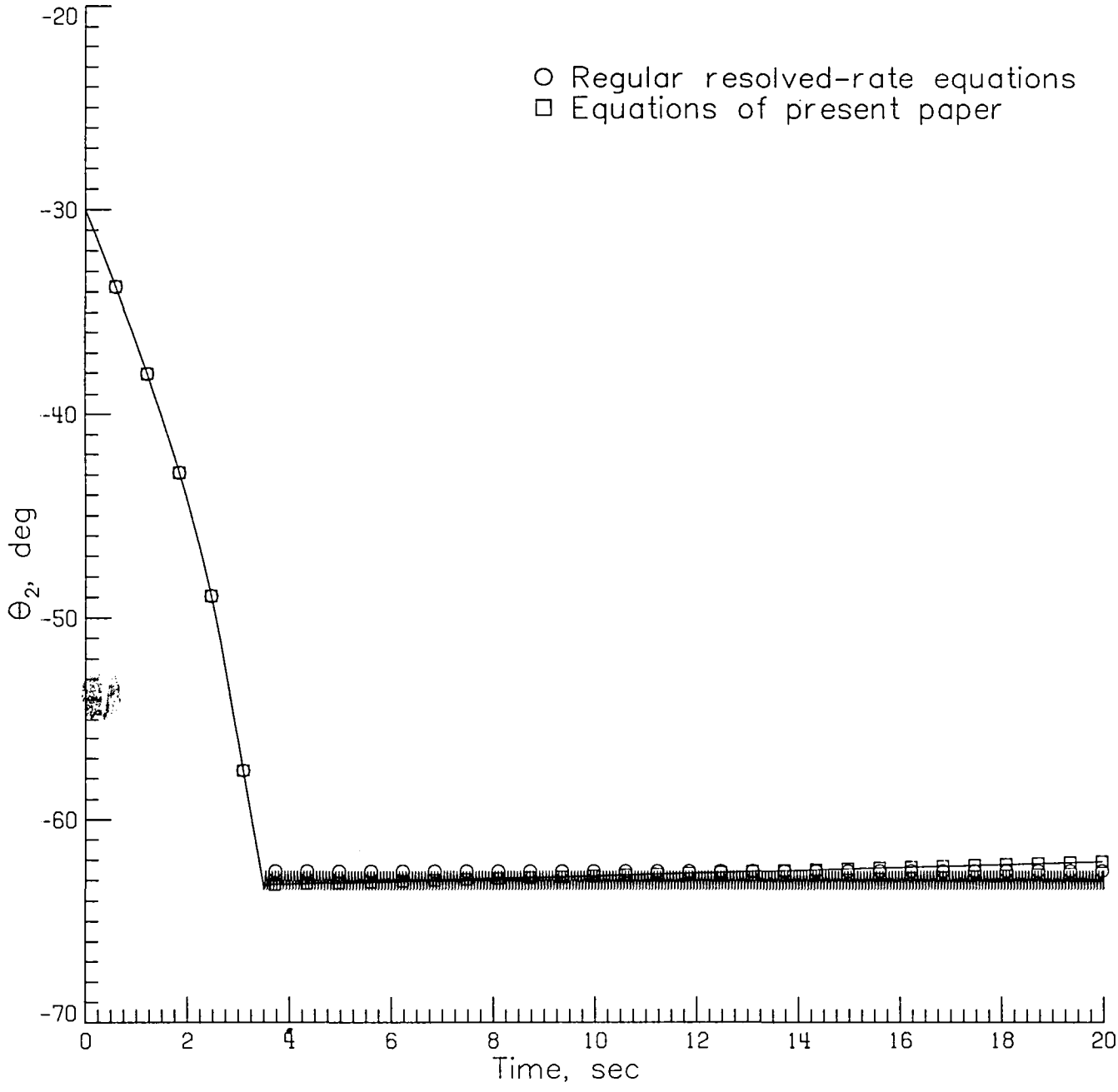

(a) Joint angle θ_2 movement.

Figure 9.- Joint angle movement for extension maneuver.

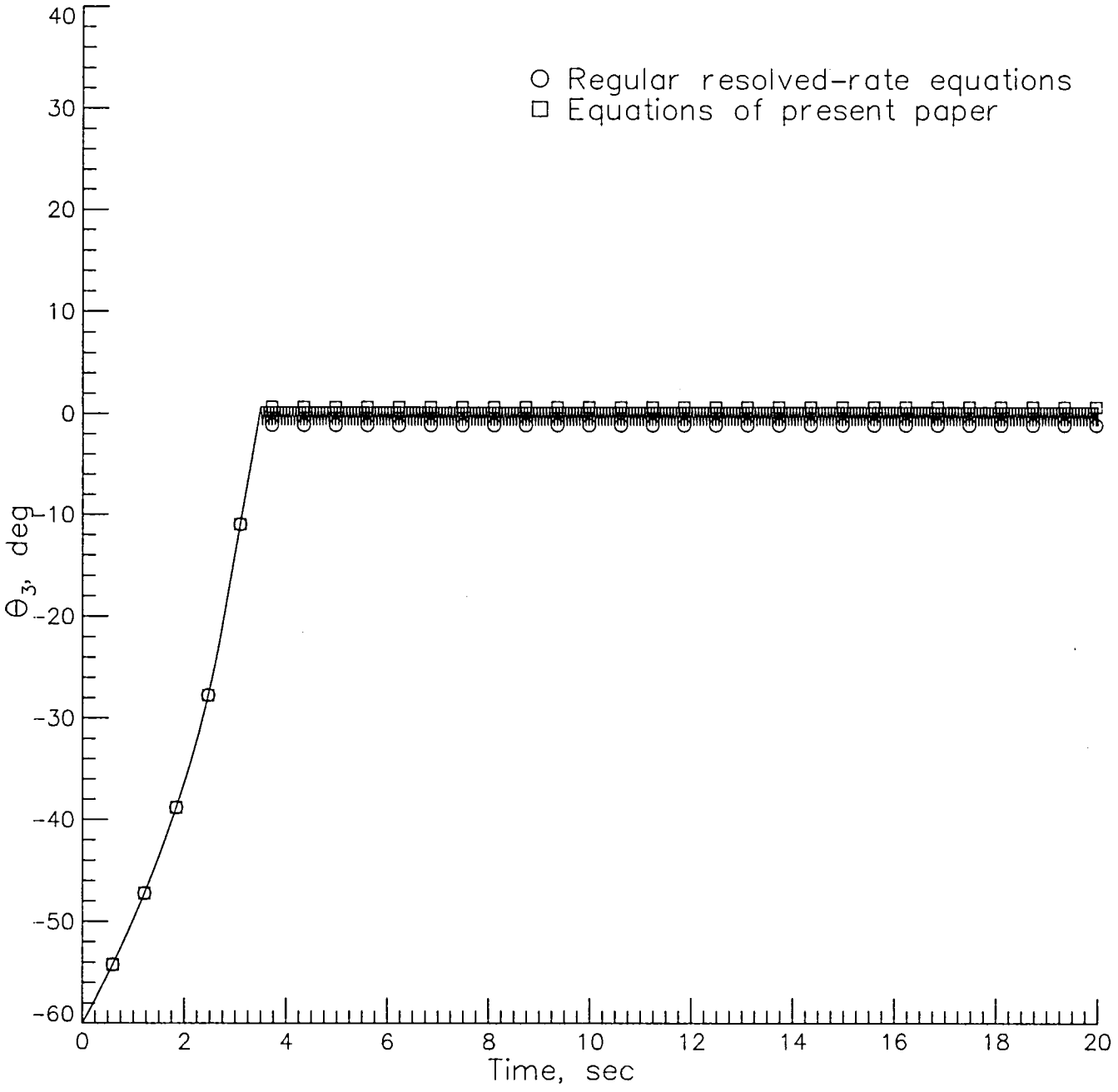

(b) Joint angle θ_3 movement.

Figure 9.- Concluded.

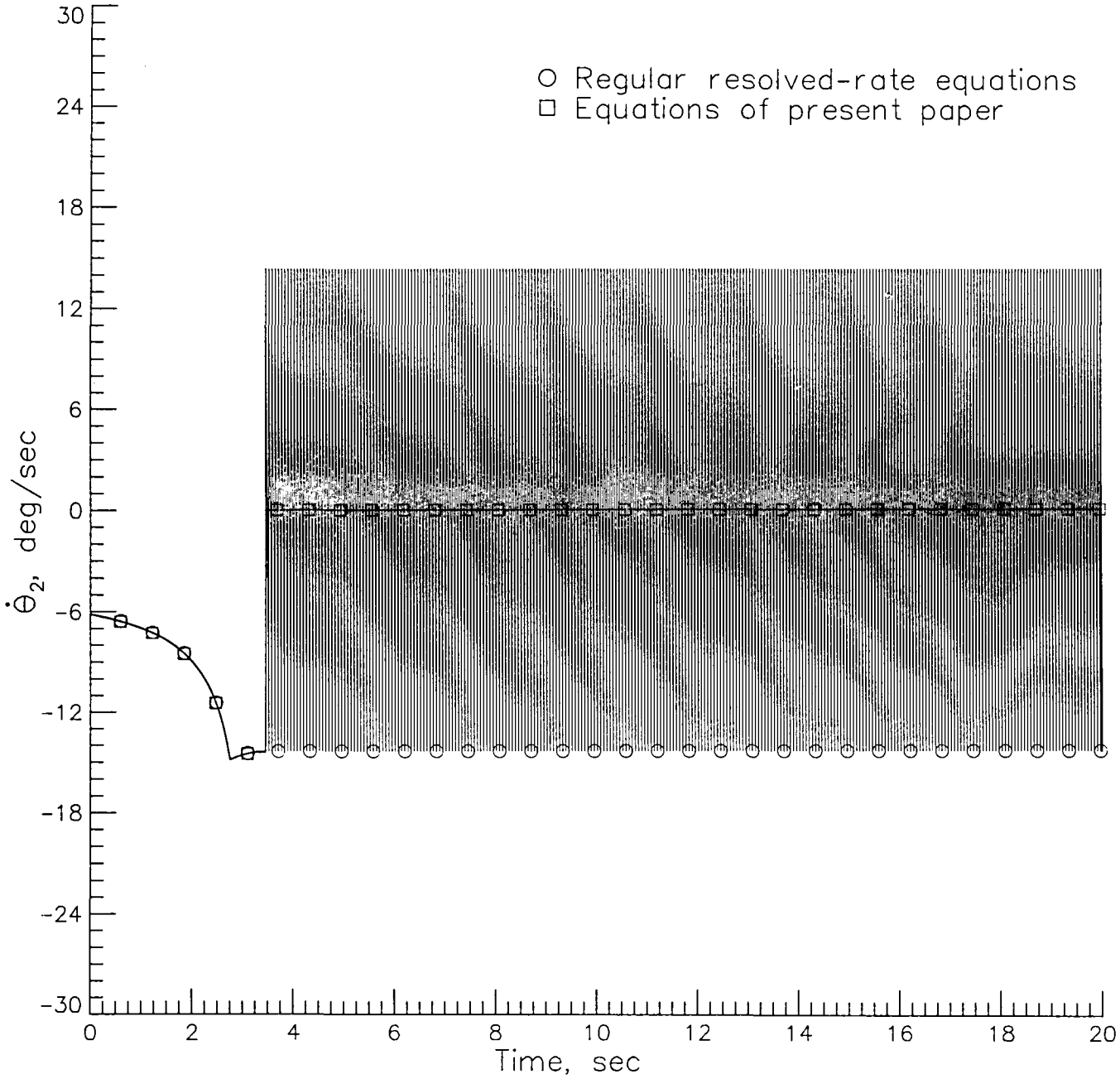

(a) Joint angle rate $\dot{\theta}_2$.

Figure 10.- Joint angle rate for extension maneuver.

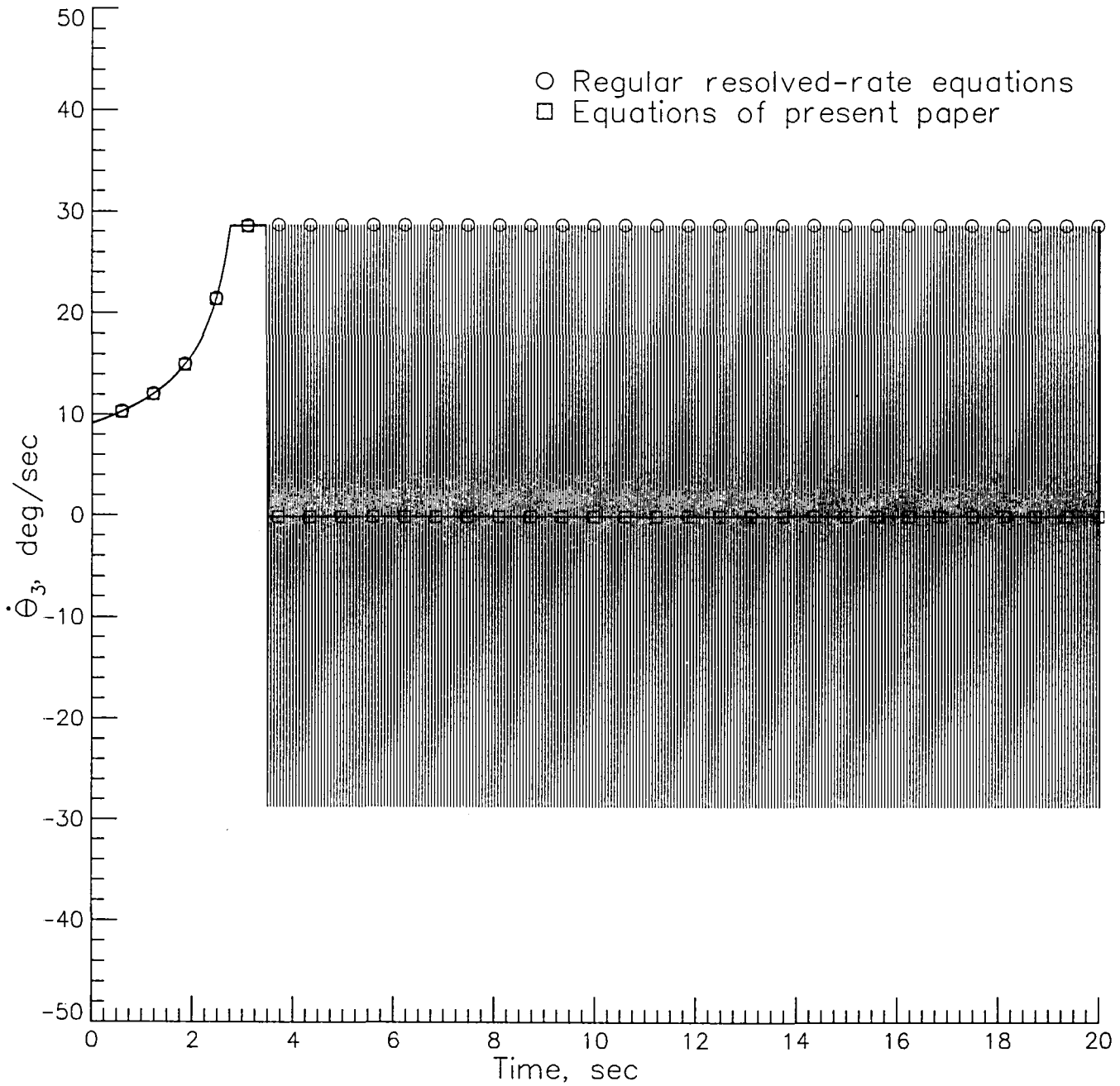

(b) Joint angle rate $\dot{\theta}_3$.

Figure 10.- Concluded.

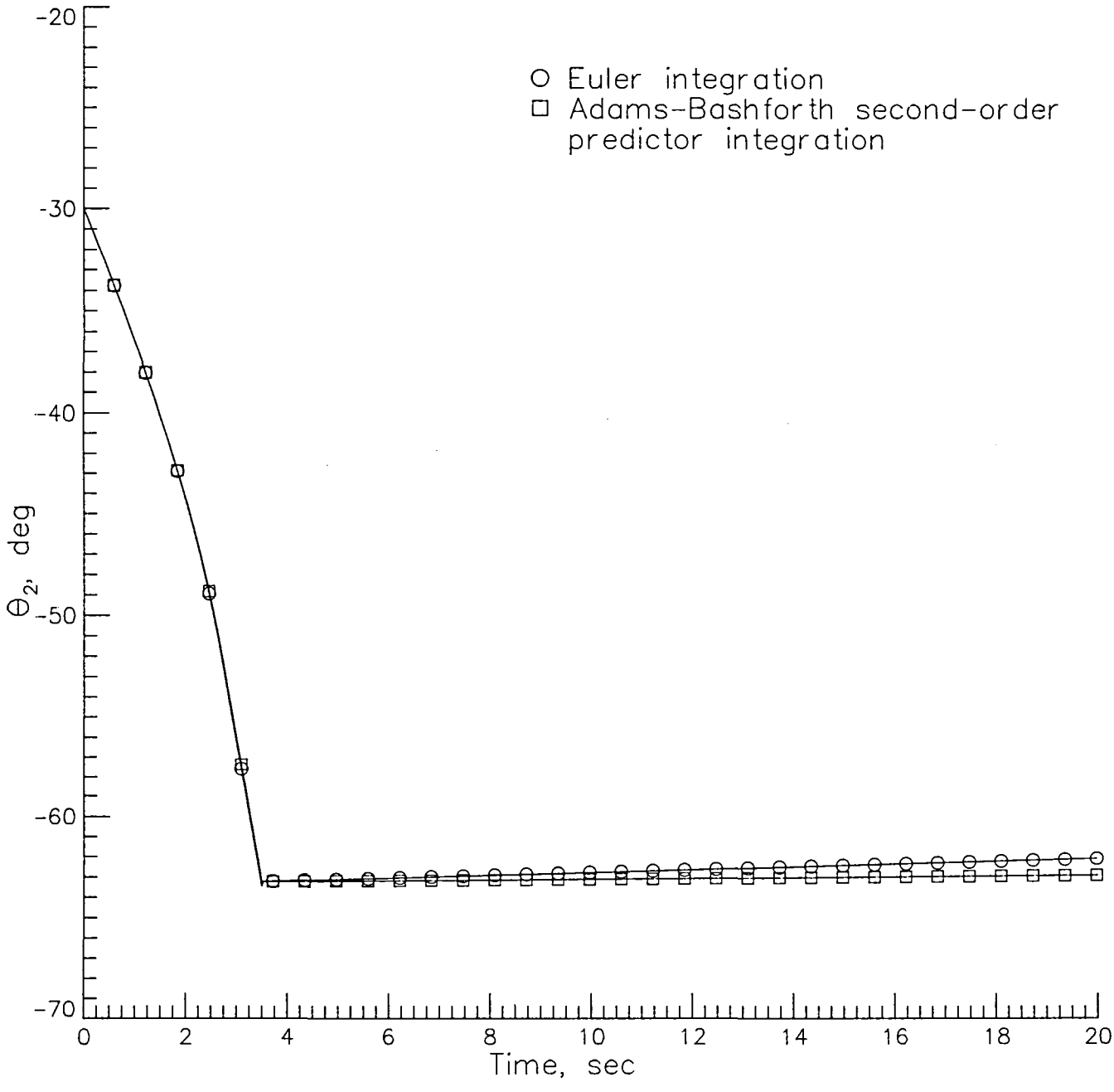

(a) Joint angle θ_2 movement.

Figure 11.- Comparison of integration schemes for extension maneuver. h = 1/32 sec.

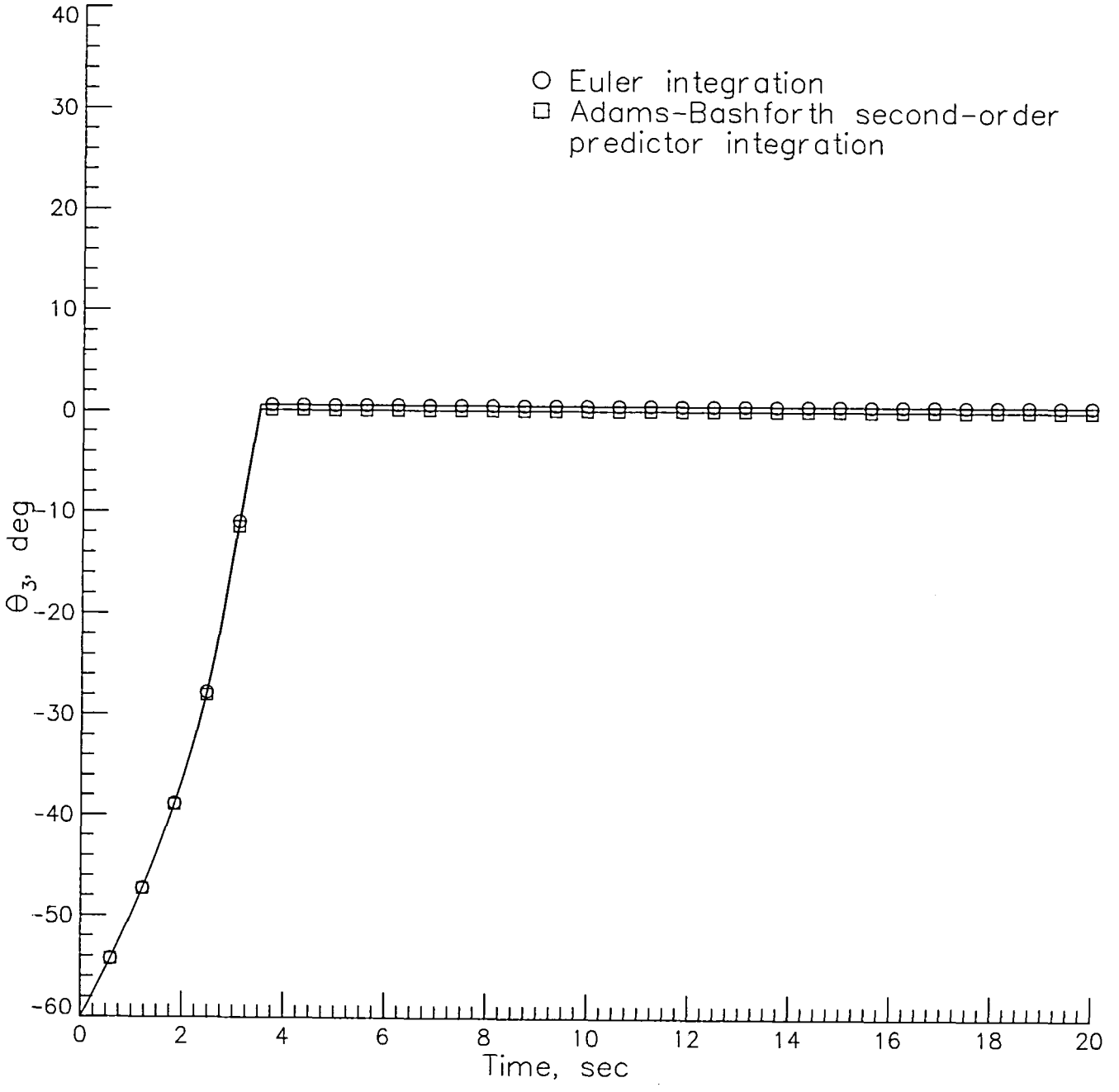

(b) Joint angle θ_3 movement.

Figure 11.- Continued.

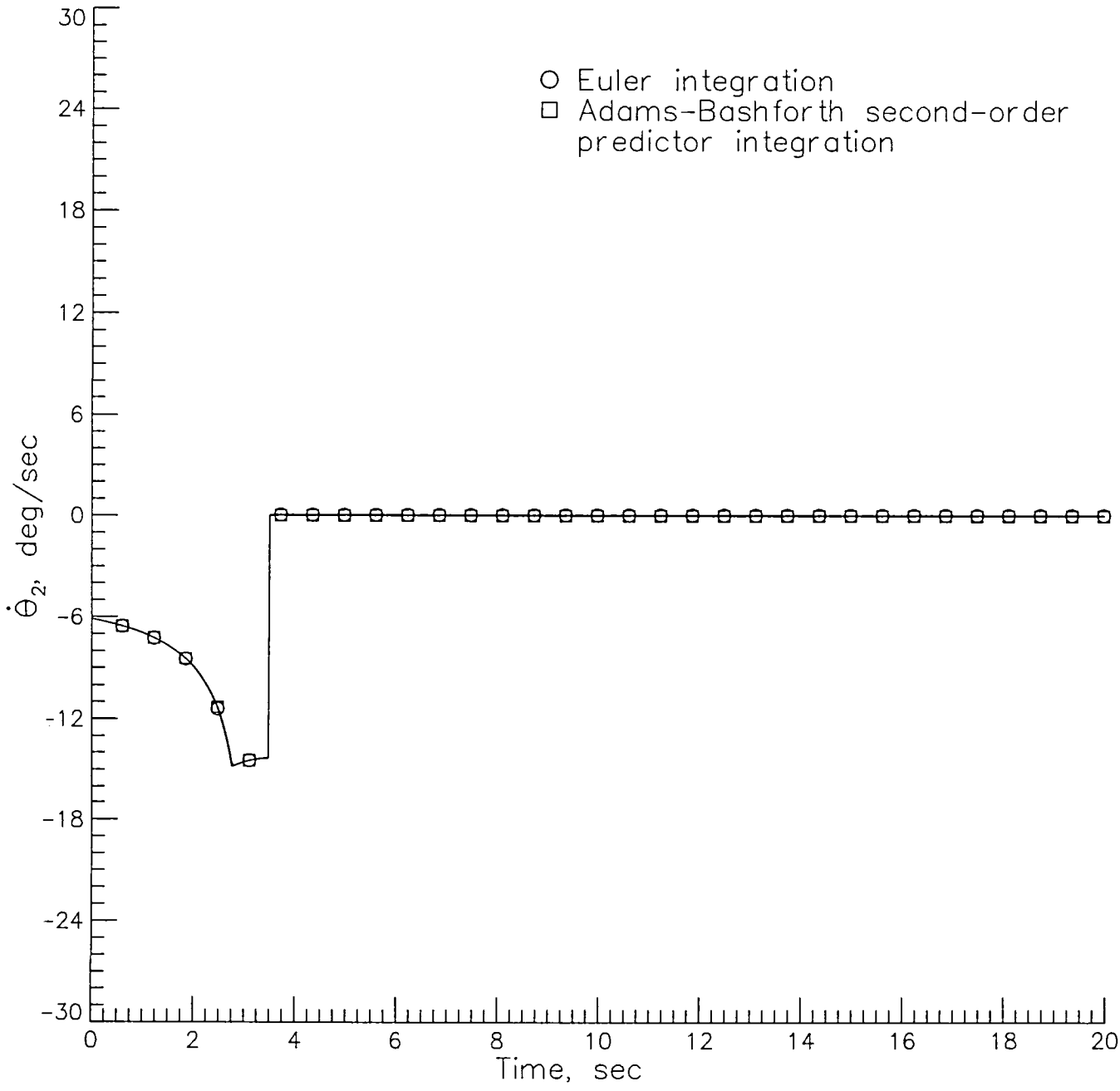

(c) Joint angle rate $\dot{\theta}_2$.

Figure 11.- Continued.

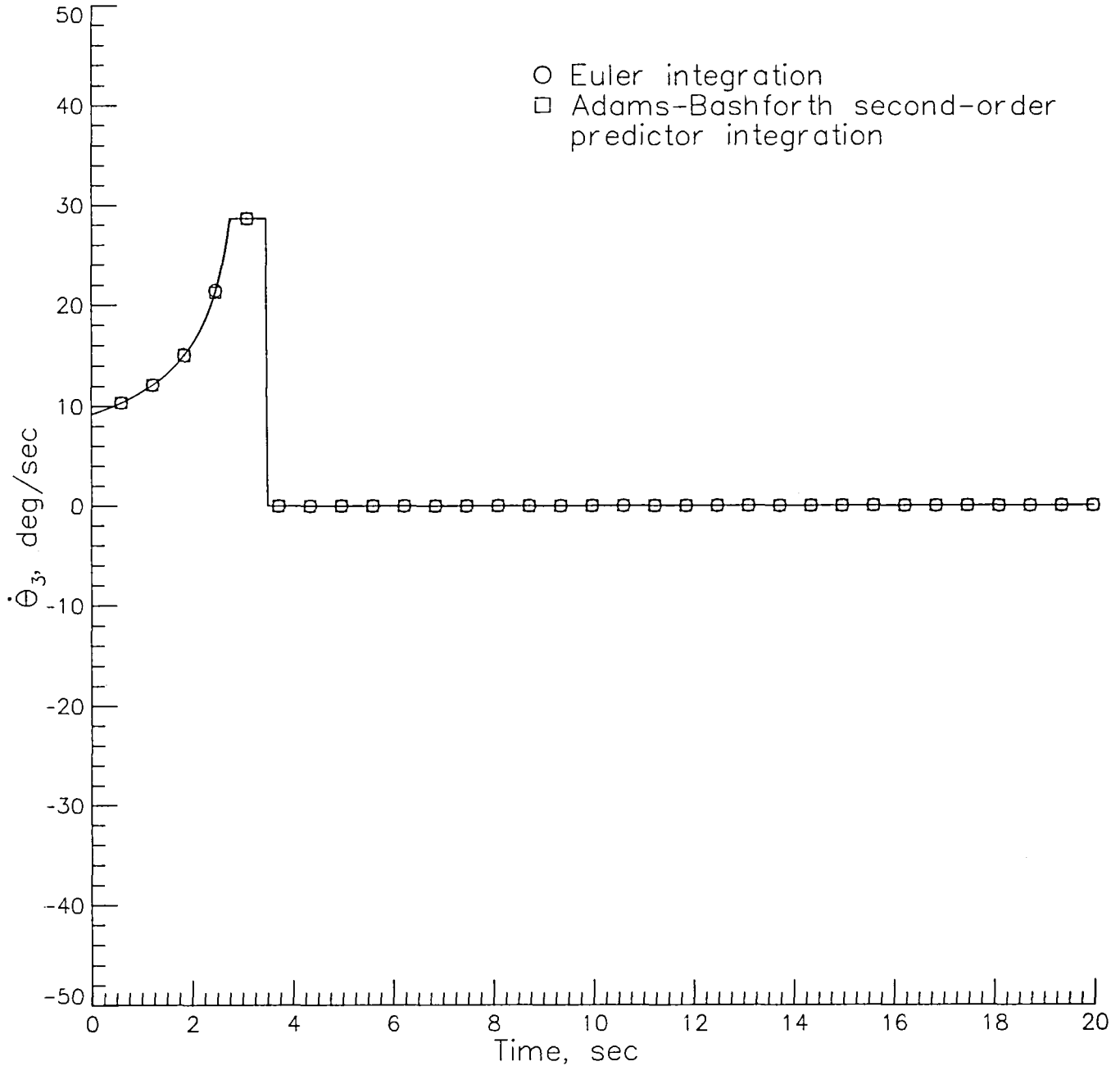

(d) Joint angle rate $\dot{\theta}_3$.

Figure 11.- Concluded.

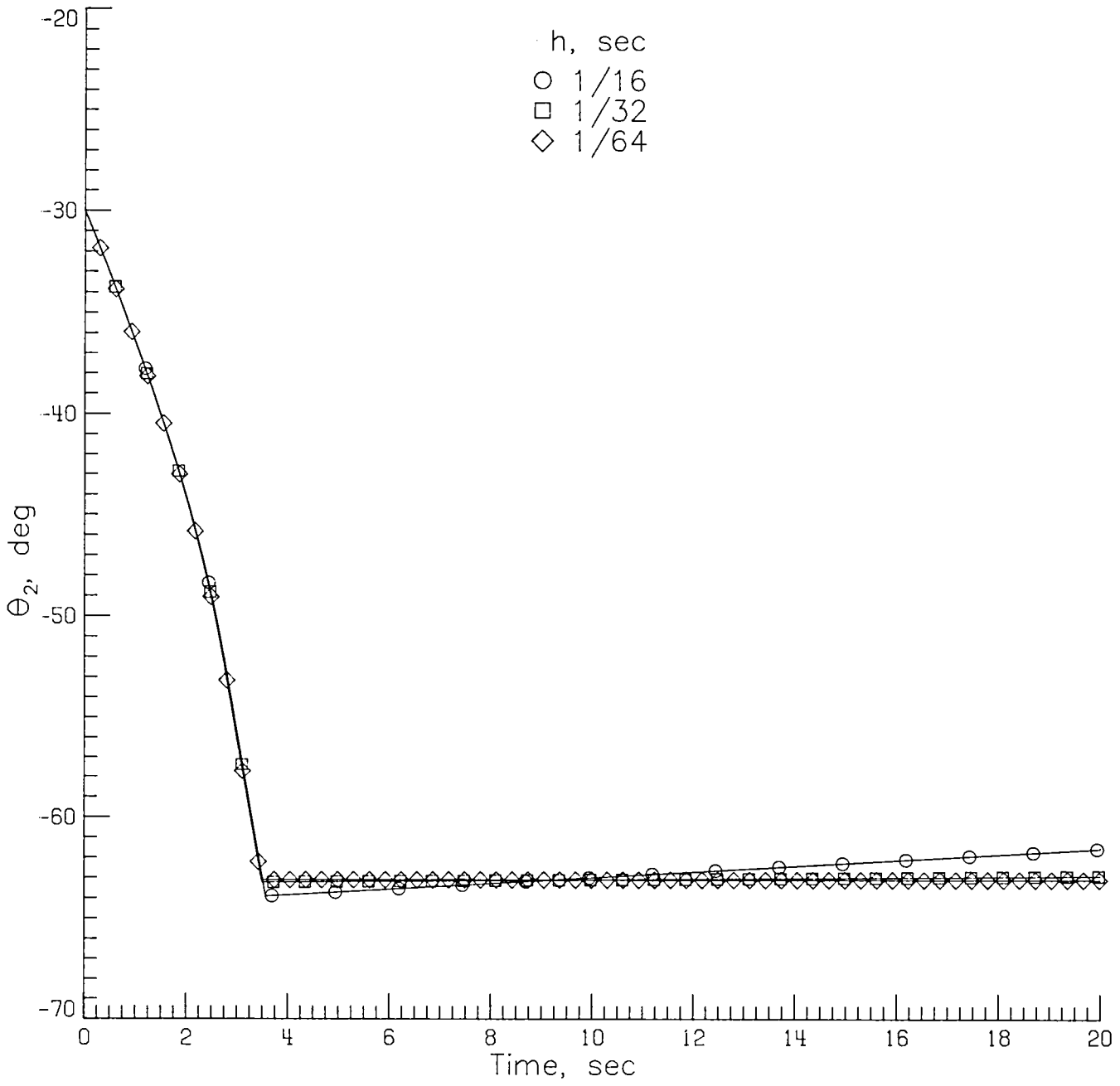

(a) Joint angle θ_2 movement.

Figure 12.- Step size comparison with Euler integration scheme for extension maneuver.

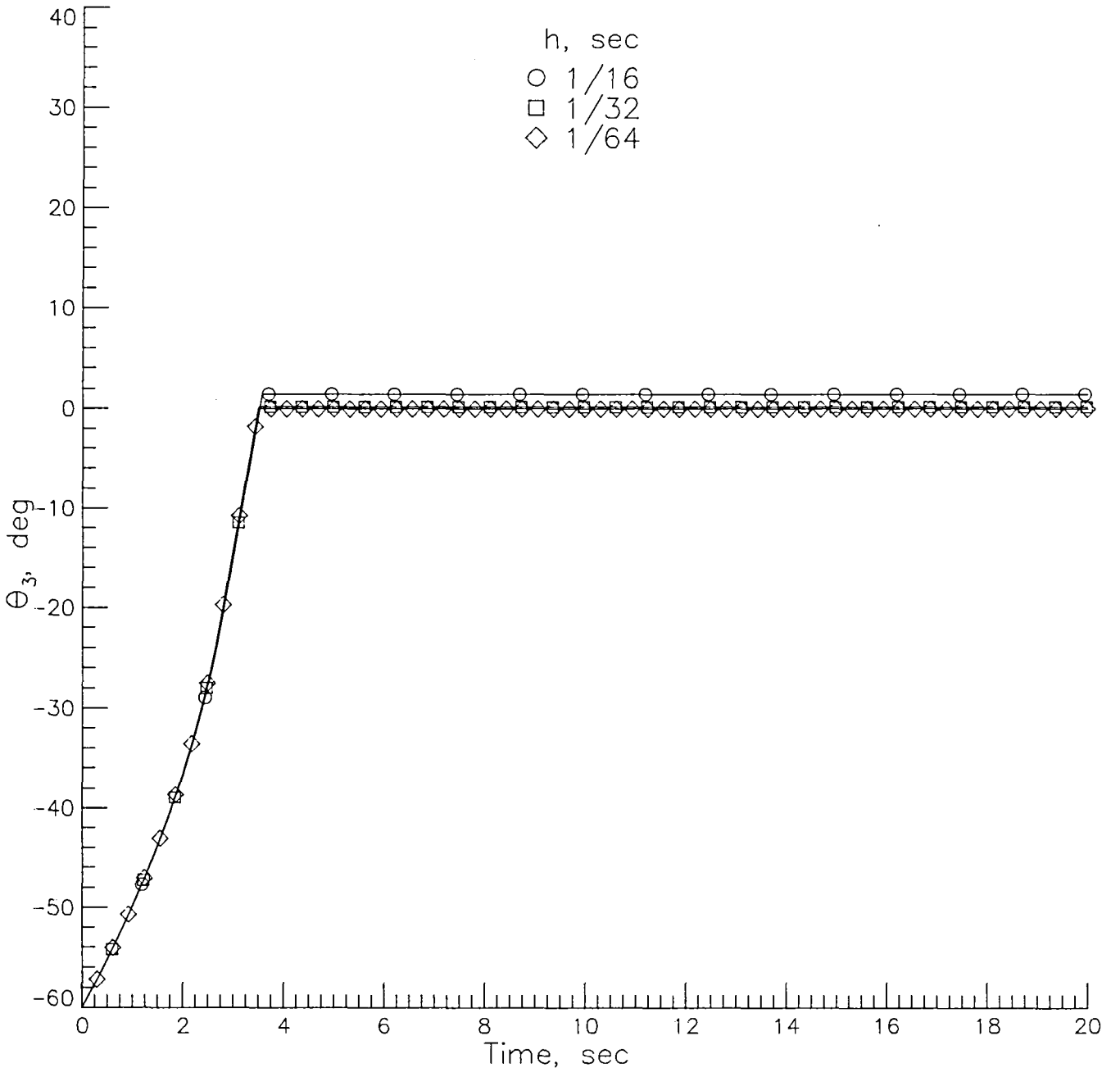

(b) Joint angle θ_3 movement.

Figure 12.- Continued.

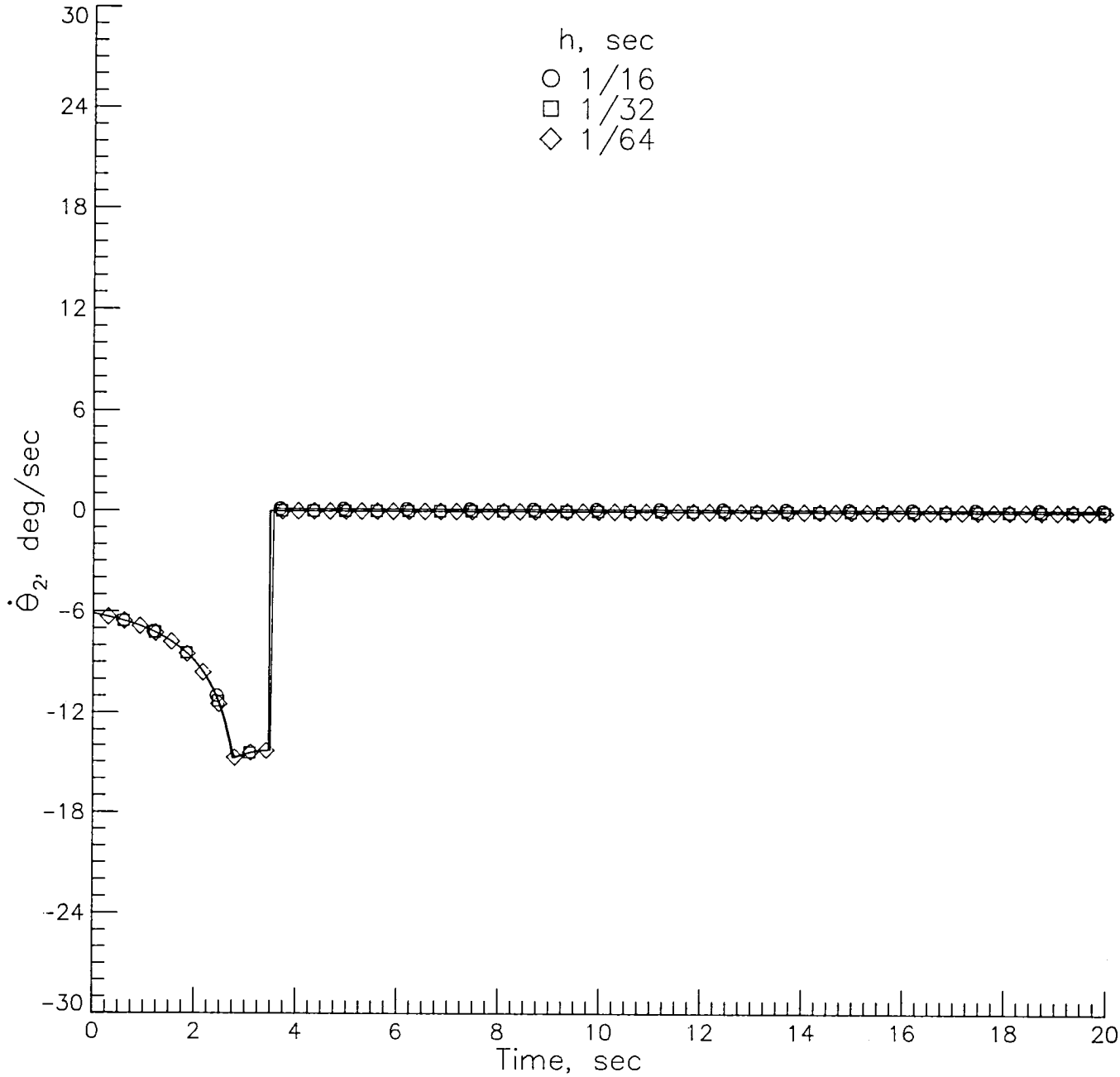

(c) Joint angle rate $\dot{\theta}_2$.

Figure 12.- Continued.

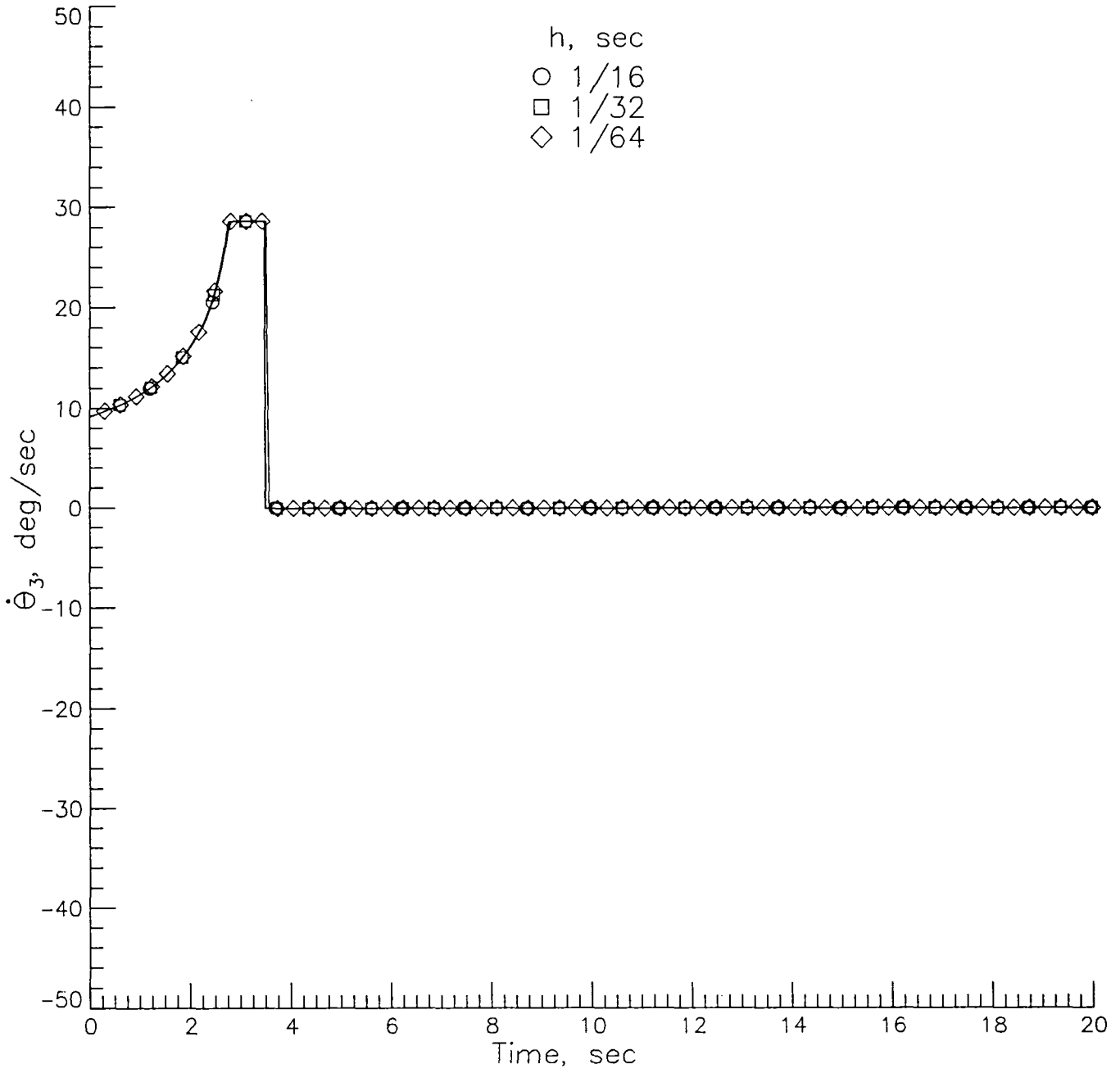

(d) Joint angle rate $\dot{\theta}_3$.

Figure 12.- Concluded.

1. Report No.	2. Government Accession No.	3. Recipient's Catalog No.
NASA TP-2376		

4. Title and Subtitle	5. Report Date
TRANSLATIONAL CONTROL OF A GRAPHICALLY SIMULATED ROBOT ARM BY KINEMATIC RATE EQUATIONS THAT OVERCOME ELBOW JOINT SINGULARITY	December 1984
	6. Performing Organization Code: 506-54-63-01-00
7. Author(s): L. Keith Barker, Jacob A. Houck, and Susan W. Carzoo	8. Performing Organization Report No.: L-15828
	10. Work Unit No.
9. Performing Organization Name and Address: NASA Langley Research Center, Hampton, VA 23665	11. Contract or Grant No.
	13. Type of Report and Period Covered: Technical Paper
12. Sponsoring Agency Name and Address: National Aeronautics and Space Administration, Washington, DC 20546	14. Sponsoring Agency Code

15. Supplementary Notes

L. Keith Barker and Jacob A. Houck: Langley Research Center, Hampton, Virginia.
Susan W. Carzoo: Sperry Corporation, Hampton, Virginia.

16. Abstract

An operator commands a robot hand to move in a certain direction relative to its own axis system by specifying a velocity in that direction. This velocity command is then resolved into individual joint rotational velocities in the robot arm to effect the motion. However, the usual resolved-rate equations become singular when the robot arm is straightened. To overcome this elbow joint singularity, equations are presented in this paper to allow continued translational control of the robot hand even though the robot arm is (or is nearly) fully extended. A feature of the equations near full arm extension is that an operator simply extends and retracts the robot arm to reverse the direction of the elbow bend (a difficult maneuver for the usual resolved-rate equations). Results show successful movement of a graphically simulated robot arm.

17. Key Words (Suggested by Author(s))		18. Distribution Statement
Robot arm	Singularities	Unclassified - Unlimited
Manipulator	Teleoperator	
Kinematic equations	Simulation	
Resolved-rate control		Subject Category 63

19. Security Classif. (of this report)	20. Security Classif. (of this page)	21. No. of Pages	22. Price
Unclassified	Unclassified	42	A03

For sale by the National Technical Information Service, Springfield, Virginia 22161 NASA-Langley, 1984

National Aeronautics and
Space Administration

Washington, D.C.
20546

Official Business
Penalty for Private Use, $300

THIRD-CLASS BULK RATE

Postage and Fees Paid
National Aeronautics and
Space Administration
NASA-451

NASA

POSTMASTER: If Undeliverable (Section 158
Postal Manual) Do Not Return